

UNIVERSITY OF NAPLES FEDERICO II



**PH.D. PROGRAM IN
CLINICAL AND EXPERIMENTAL MEDICINE
*CURRICULUM IN TRANSLATIONAL MEDICAL SCIENCES***

XXX Cycle
(Years 2014-2017)

Chairman: Prof. Gianni Marone

PH.D. THESIS

**LPS-elicited TSLPR Expression Enriches a Functionally
Discrete Subset of Human CD14⁺ CD1c⁺ Monocytes**

TUTOR

Prof. Gianni Marone

PH.D. STUDENT

Dr. Raffaella Iannone

Abstract

Thymic stromal lymphopoietin (TSLP) is a cytokine produced mainly by epithelial cells in response to inflammatory or microbial stimuli and binds to the TSLP receptor complex, a heterodimer composed of TSLP receptor (TSLPR) and IL-7 receptor α (CD127). TSLP activates multiple immune cell subsets expressing the TSLP receptor complex and plays a role in several models of disease. Although human monocytes express *TSLPR* and *CD127* mRNAs in response to the TLR4 agonist LPS, their responsiveness to TSLP is ill-defined. We demonstrate that TSLP enhances human CD14 $^{+}$ monocyte CCL17 production in response to LPS and IL-4. Surprisingly, only a subset of CD14 $^{+}$ CD16 $^{-}$ monocytes (TSLPR $^{+}$ mono) expresses TSLP receptor complex upon LPS stimulation in an NF- κ B- and p38-dependent manner. Phenotypic, functional and transcriptomic analysis revealed specific features of TSLPR $^{+}$ mono, including higher CCL17 and IL-10 production and increased expression of genes with important immune functions (i.e. *GAS6*, *ALOX15B*, *FCGR2B*, *LAIR1*). Strikingly, TSLPR $^{+}$ mono express higher levels of the dendritic cell marker CD1c. This evidence led us to identify a subset of peripheral blood CD14 $^{+}$ CD1c $^{+}$ cells that expresses the highest levels of TSLPR upon LPS stimulation. The translational relevance of these findings is highlighted by the higher expression of *TSLPR* and *CD127* mRNAs in monocytes isolated from patients with Gram-negative sepsis compared to healthy controls. Our results emphasize a phenotypic and functional heterogeneity in an apparently homogeneous population of human CD14 $^{+}$ CD16 $^{-}$ monocytes and prompt further ontogenetic and functional analysis of CD14 $^{+}$ CD1c $^{+}$ and LPS-activated CD14 $^{+}$ CD1c $^{+}$ TSLPR $^{+}$ monocytes.

Table of contents

1. Introduction	1
1.1. Thesis: an overview and aim of the project	1
1.2. The immune system	2
1.2.1. Monocytes	3
1.3. Thymic stromal lymphopoietin	4
1.3.1. TSLP as potential therapeutic target	4
2. Materials and methods	6
2.1. Cell isolation and culture	6
2.2. ELISA	6
2.3. Flow and imaging cytometry	7
2.4. Fluorescence-activated cell sorting (FACS)	8
2.5. Mixed leucocyte reaction (MLR)	8
2.6. Time-lapse microscopy	8
2.7. RNA isolation and real time RT-PCR	9
2.8. RNA-sequencing and bioinformatic analysis	9
2.9. Accession number	10
2.10. Statistical analysis	11
3. Results	12
3.1. TSLP enhances human monocytes production of CCL17	12
3.2. TLR4 activation elicits a subset of human TSLPR ⁺ monocytes that preferentially originates from CD16 ⁻ monocytes	12
3.3. TLR4-activated signaling pathways required for the induction of TSLPR ⁺ monocytes	13
3.4. TSLPR ⁺ monocytes exhibits discrete phenotypic and functional features	14

3.5. TSLP is preferentially expressed by a subset of CD14 ⁺ CD1c ⁺ monocytes	16
3.6. In vivo monocyte expression of TSLPR and CD127 in Gram-negative sepsis	17
4. Discussion	18
5. Figure legends	21
6. References	62

1. Introduction

1.1 Thesis: an overview and aim of the project

Thymic stromal lymphopoitin (TSLP) is a cytokine produced mainly by epithelial cells in response to inflammatory or microbial stimuli ⁽¹⁾. TSLP binds to the TSLP receptor complex, a heterodimer composed of TSLP receptor (TSLPR) and interleukin (IL)-7 receptor α (IL-7R- α or CD127), and activates several signaling pathways, including the Janus kinase/signal transducer and activator of transcription (JAK-STAT5) pathway ⁽²⁾. TSLP receptor complex is expressed by epithelial cells and also several immune cell subsets, including dendritic cells (DCs). Importantly, several lines of evidence support a model in which TSLP activation of DCs results in Th2 differentiation *in vitro* and type 2 immunity *in vivo* ^(3, 4). As such, TSLP has been involved in the development of atopic diseases, tissue remodeling and in the modulation of the immune response to ectoparasite infections and cancers ^(1, 5). Nevertheless, the breadth of TSLP activity is not limited to type 2 immunity-related conditions. For example, TSLP is expressed in psoriatic lesions and instructs CD40 ligand (CD40L)-activated DCs to produce IL-12 and IL-23, which play a central role in psoriasis pathogenesis ^(6, 7). This cytokine has also been implicated in the pathogenesis of rheumatic diseases, at least in part by activating DCs ⁽⁸⁾. Finally, TSLP dampens myeloid cell inflammatory response in an experimental model of sepsis ⁽⁹⁾. Thus, understanding the response of myeloid cells (i.e. DCs, macrophages, neutrophils and monocytes) to TSLP may be relevant for several physiologic and pathologic conditions. Although human monocytes stimulated with lipopolysaccharide (LPS), the major component of the outer membrane of Gram-negative bacteria, express *TSLPR* and *CD127* mRNAs ⁽¹⁰⁾, their responsiveness to TSLP is ill-defined.

Activation of DCs with TSLP induces several phenotypic and functional responses, including the production of the chemokine CCL17/Thymus and activation regulated chemokine (TARC) that promotes the recruitment of CCR4-expressing cells (e.g. T helper [Th] 2 and regulatory T [Treg] lymphocytes) ⁽¹⁾. Monocytes and macrophages activated with IL-4 or IL-13 also produce CCL17 in a STAT6-dependent manner ^(11, 12). Interestingly, TSLP and IL-4 or IL-13 synergize to induce CCL17 production by mouse macrophages ⁽¹³⁾. We have shown that the STAT5-activating cytokines IL-3 and GM-CSF synergize with IL-4 to enhance CCL17 production by human monocytes and macrophages ⁽¹⁴⁾. Since TSLP activates STAT5, we reasoned that also TSLP could enhance CCL17 production by human monocytes activated with LPS and IL-4. By investigating human monocyte responsiveness to TSLP, we

unexpectedly found that only a subset of human CD14⁺ monocytes express the TSLP receptor complex upon LPS stimulation and proceeded to characterize this subset. We demonstrate that TSLPR⁺ monocytes express distinct phenotypic, functional and transcriptomic profiles compared to TSLPR⁻ monocytes, and are also enriched for a subset of CD14⁺ CD1c⁺ monocytes. The translational relevance of these findings is highlighted by the higher expression of *TSLPR* and *CD127* mRNAs in monocytes isolated from patients with Gram-negative sepsis compared to healthy controls.

1.2 The immune system

The immune system protects an organism from harmful invading pathogens, such as bacteria, viruses, fungi, parasites, and can be divided into the innate and adaptive immune system.

The innate immune system play an important role in host defense in the early stages of infection through non-specific recognition of a pathogen, while the main characteristics of adaptive immunity are specific recognition of pathogen leading to the generation of pathogen specific long-term memory ⁽¹⁵⁾. Moreover, innate immune cells (i.e. monocytes and macrophages) may be exposed to different and sometimes opposing stimuli in a sequential manner, and the priming stimulus may exert a significant control over the response to subsequent stimuli. This phenomenon, which is referred to as “innate immune memory” or “trained immunity” ^(16, 17, 18).

Innate immune cells are largely derived from myeloid hematopoietic precursors, and include neutrophils, eosinophils, basophils, macrophages, monocytes, DCs, and mast cells. A few innate (or innate-like) immune cells are derived from lymphoid hematopoietic precursors, and include natural killer (NK) cells, NKT cells, and gamma/delta ($\gamma\delta$)-T cells. The innate immune response relies on recognition of conserved structures on pathogens, termed pathogen-associated molecular patterns (PAMPs), through a limited number of germ line-encoded pattern recognition receptors (PRRs), and toll-like receptors (TLRs) is the most extensively studied class of PRRs ⁽¹⁹⁾. The different TLRs can be activated in response to different exogenous and endogenous ligands. An example is lipopolysaccharide (LPS), which binds to and activates its receptor TLR4, leading to expression of pro-inflammatory factors such as the cytokine tumor necrosis factor (TNF)- α ⁽²⁰⁾.

Adaptive immunity is largely mediated by T and B cells, acting through pathogen-specific surface receptors (T cell receptor [TCR] and B cell receptor [BCR], respectively). B cells are responsible for secreting antibodies, while T cells mediate more cellular effector responses (**Figure 1**)⁽²¹⁾.

1.2.1 Monocytes

Monocytes are innate immune cells that circulate in the blood, bone marrow, and spleen and migrate from blood to tissues during infection⁽²²⁾.

They are members of the mononuclear phagocyte system, a family of myeloid cells that comprises monocytes, DCs and macrophages. Human monocytes are distinguished by their surface expression of CD14 (migratory monocytes) and CD16 (patrolling monocytes), and three human cell subsets can be characterized, namely classical CD14⁺⁺CD16⁻, intermediate CD14⁺⁺CD16⁺ and non-classical CD14⁺CD16⁺⁺ monocytes^(23, 24). The classical and intermediate subsets were most closely related among the subsets, while the non-classical subset was the most distant subset.

Circulating monocytes exhibit a diameter of approximately 7–8 µm. However, monocytes can mature into macrophages during inflammation and injury and reach diameters of 15–20 µm. In response to infection, inflammation or tumor, monocytes, called "inflammatory monocytes", rapidly emigrate into tissue, and there acquire a wide variety of properties that are specifically associated with the local processes that led to their accumulation. Monocyte-derived macrophages are commonly classified into "pro-inflammatory" (M1-like) and "pro-resolving" or "anti-inflammatory" (M2-like)⁽²⁵⁾.

Monocytes can differentiate also into DCs. Dermal CD14⁺ DCs, and intestinal CD103⁻CD172a⁺ DCs potentially represent populations of monocyte-derived cells. In inflamed tissues, the "inflammatory DCs" expressing CD1c, CD1a and CD14 are also likely to be monocyte-derived cells^(26, 27, 28, 29, 30).

1.3 Thymic stromal lymphopoietin

TSLP is an epithelial derived cytokine, whose gene is located on chromosome 5q22.1, and it exerts its biological function through TSLP receptor complex that consists of a unique common γ (γ c) chain-like TSLP receptor and the IL-7 receptor α chain ⁽²⁾. The TSLP receptor complex is expressed by hematopoietic cells, including T cells, B cells, NKT cells, macrophages, basophils, DCs, as well as some non-hematopoietic cell lineages, such as epithelial cells, suggesting that TSLP can act on a wide range of cell types. In fact, TSLP activates several immune cell subset, especially DCs, and induces Th2 differentiation and type 2 immunity *in vitro* and *in vivo*.

TSLPR has low affinity for TSLP, but in combination with IL-7R α generates a high-affinity binding site for TSLP and triggers signaling through signal transducer and activator of transcription STAT1, STAT3, STAT5 and JAK1 and JAK2 (**Figure 3**) ⁽¹⁾.

However, freshly isolated human monocytes don't express TSLPR complex. Human TSLPR and CD127 are co-expressed on monocytes only upon stimulation with LPS (**Figure 4**) ⁽¹⁰⁾.

1.3.1 TSLP as potential therapeutic target

TSLP genetic variants and its dysregulated expression have been linked to atopic diseases (e.g. atopic dermatitis [AD], asthma), but also to other immune-mediated diseases such as cancer and rheumatoid arthritis ⁽³¹⁾.

In approximately 10–60% of patients with B-cell acute lymphoblastic leukemias (ALL) and in some with T-ALL, there are somatic gain-of-function mutations in TSLP-R associated with the aberrant expression of TSLPR α and mutant CD127 proteins have formed a functional receptor TSLP ^(31, 32).

Abnormally high expression of TSLP gene was observed in AD patients. Clinical trial assessing effectiveness of tezepelumab (AMG 157), a fully human anti-TSLP monoclonal antibody that specifically binds human TSLP preventing interaction with its receptor, in comparison to placebo in patients with severe AD has been completed ⁽³³⁾.

Tezepelumab also demonstrated improvements in lung function, and significantly reduced asthma exacerbations for patients with severe uncontrolled asthma ⁽³⁴⁾. In addition, Tezepelumab reduced eosinophil counts and fractional exhaled nitric oxide concentrations

before allergen challenge, suggesting that TSLP is constitutively released in the airways of allergic asthmatic, and its blockade may provide similar clinical benefit to blockade of Th2 cytokines, such as IL-5 and IL-3^(35, 36).

2. Materials and methods

2.1. Cell isolation and culture

The study protocol involving the use of human blood cells was approved by the Ethics Committee of the University of Naples Federico II. Cells were isolated from buffy coats of healthy donors. Blood was layered onto Histopaque-1077 (Sigma-Aldrich) and mononuclear cells were collected at the interface. Monocytes were further purified with CD14 Microbeads (Miltenyi Biotec). Purity of cell preparations was > 95% as assessed by flow cytometry (CD14⁺ cells). Cells were cultured in cIMDM-5 (IMDM, 5% FCS, 1x non essential amino acids, 1x UltraGlutamine, 25 mM HEPES, 5 µ/ml gentamicin [Lonza]) in 96-well flat-bottom plates (10^5 monocytes/well) in a final volume of 250 µl. For experiments involving flow cytometry or fluorescence-activated cell sorting (FACS), cells were cultured in suspension (1.5 ml tubes for flow cytometry, 50 ml tubes for FACS) at a concentration not greater than 2×10^6 cells/ml, then spun down and collected for the subsequent staining protocols. For experiments aimed at evaluating the modulation of TSLP receptor complex expression, cells were cultured in cIMDM-0.5 (0.5% FCS).

Cells were treated with different combinations of: LPS (*E. coli* O26:B6) 10, 100 and 1000 ng/ml, phytohemagglutinin (PHA) 10 µg/ml (Sigma), IL-4 10 ng/ml, TSLP 5 ng/ml (Miltenyi Biotec), anti-human TNF-α 1 µg/ml, mouse IgG1 κ isotype control 1 µg/ml (eBioscience), P3CSK4 10, 100 and 1000 ng/ml, Poly(I:C) 1 µg/ml, flagellin 10 ng/ml, imiquimod 1 µg/ml, ODN2006 1 µM, HKPA, HKSA and HKEB (monocytes:bacteria ratio 1:10) (Invivogen), BAY11-7082 0.5, 1 and 2 µM, SP600125 2 µM, CHIR-98014 200 nM, Wortmannin 1 µM (Selleckchem), UO126 2 µM, LY294002 10 µM, SB203580 2 µM (Cell Signaling Technology).

2.2. ELISA

Cytokine concentrations were measured in cell-free supernatants using commercially available ELISA kits for CCL17 (R&D Systems), TNF-α, IL-1β, IL-6 and IL-10 (eBioscience). Briefly, 96-well plates (NUNC) were coated with capture antibody diluted in PBS. The plates were then washed in PBS containing 0.05% Tween-20 (PBST), and blocked with PBS+BSA 1%, before the incubation with standards and samples. The plates were then washed in PBST before incubation with the secondary antibody. The plates were then washed

in PBST before the addition of detection antibody. The plates were washed in PBST and Streptavidin-HRP was added. Then, the plates were washed in PBST before the addition of tetramethylbenzidine. The reaction was stopped with H₂SO₄ and a microplate reader (TECAN infinite 200 pro) was used to determine sample absorbance at 450 nM.

Standard curves were generated with a Four Parametric Logistic curve fit and data were analysed using MyAssays Analysis Software Solutions (www.myassays.com).

2.3. Flow and imaging cytometry

Flow and imaging cytometry experiments were performed with purified monocytes. For surface staining, cells were stained (20 minutes at 4°C) in PBS + 10% human AB serum (Lonza) + 0.05% NaN₃ (Staining buffer, SB). For phosphoprotein staining, cells were rested in cIMDM-0.5 for 1 hour and stimulated with the indicated cytokines for 15 minutes. Then, cells were fixed with paraformaldehyde (EM-grade, Electron Microscopy Sciences) (final concentration 1.5%) and permeabilized with absolute ice-cold methanol. Cells were stained (30 minutes at room temperature) in SB. The following antibodies were used: anti-human-phospho-STAT5 AlexaFluor 647 (clone 47, dilution 1:20), anti-human-TSLPR APC (clone 1A6, dilution 1:40) (BD Biosciences), anti-human-CD127 PE-Vio770 (clone MB15-18C9, dilution 1:20), anti-human-CD14 FITC (clone TÜK4, dilution 1:20), anti-human-CD16 PE (clone VEP13, dilution 1:20), anti-human-CD11b PE (clone M1/70.15.11.5, dilution 1:20), anti-human-CD11c PE (clone REA618, dilution 1:20), anti-human-HLA-DR PE (clone REA332, dilution 1:20), anti-human-CD1c PE (clone AD5-8E7, dilution 1:20) (Miltenyi Biotec). For flow cytometry experiments, samples were acquired on MACSQuant Analyzer 10 (Miltenyi Biotec) and analyzed using FlowJo v10. Doublets, debris (identified based on forward and side scatter properties) and dead cells (identified with Zombie Violet Fixable Viability Kit [Biolegend]) were excluded from the analysis. Data are expressed as percentage of positive cells and median fluorescence intensity (MFI). For imaging cytometry experiments, samples were acquired on Amnis ImageStream^x Mark II (EMD Millipore).

Unfocused cells and doublets were excluded from the analysis and representative images were taken in the following gates: TSLPR⁺ CD127⁺ and TSLPR⁻ CD127⁺ cells.

2.4. Fluorescence-activated cell sorting (FACS)

For sorting of CD14^{hi} CD16⁻ and CD14⁺ CD16⁺ cells, monocytes were left untreated and stained with anti-CD14 and anti-CD16 antibodies. For sorting of TSLPR⁺ cells, monocytes were cultured for 14 hours as indicated above and then stained with anti-TSLPR. Staining were performed in PBS + 10% human AB serum (Lonza) for 30 minutes at 4°C, then cells were washed with PBS + 0.2% BSA, filtered (pre-separation filters [70 µm], Miltenyi Biotec) and sorted through a BD FACSARIA III (BD Biosciences). Purity of sorted cells was > 90%.

The following antibodies were used to stain 20 – 30 x 10⁶ monocytes: anti-human-TSLPR APC (clone 1A6, dilution 1:20) (BD Biosciences), anti-human-CD14 FITC (clone TÜK4, dilution 1:7), anti-human-CD16 PE (clone VEP13, dilution 1:8) (Miltenyi Biotec).

2.5. Mixed leukocyte reaction (MLR)

FACS-sorted TSLPR⁺ and TSLPR⁻ monocytes were stimulated for 14 hours with LPS or LPS + IL-4 in cIMDM-5. Then, cells were washed and cultured in cIMDM-5 for 7 days with CD4⁺ T lymphocytes isolated with CD4 Microbeads (Miltenyi Biotec) from unrelated donors and labeled with CFSE (5 µM, Thermo-Fischer). Unstimulated and PHA-stimulated CD4⁺ T lymphocytes labeled with CFSE were used as controls. On day 7 non-adherent cells (i.e. CD4⁺ T lymphocytes) were harvested, acquired on a MACSQuant Analyzer 10 (Miltenyi Biotec) and analyzed using FlowJo v10. Doublets, debris (identified based on forward and side scatter properties) and dead cells (identified with Zombie Violet Fixable Viability Kit [Biolegend]) were excluded from the analysis. Unstimulated CFSE-labeled CD4⁺ T lymphocytes were employed to set the gate for CFSE^{low} lymphocytes (i.e. proliferating lymphocytes).

2.6. Time-lapse microscopy

TSLPR⁺ and TSLPR⁻ monocytes were stimulated for 14 hours with LPS or LPS + IL-4 in cIMDM-5. Over this time window digital phase contrast images of 15 fields/well were taken every 15 minutes with the Operetta High-Content Imaging System (PerkinElmer). To quantify cell movements, square displacement was calculated for each cell as the sum of squared

displacement of the X and Y axes. Then, the average of square displacements was calculated to compute the mean square displacement (MSD) for each condition.

2.7. RNA isolation and real time RT-PCR

Total RNA was extracted using TRIzol reagent (Invitrogen), according to the manufacturer's protocol. For RNA-sequencing, RNA was extracted using ReliaPrep RNA Cell Miniprep System (Promega). Reverse transcription of 500 ng of total RNA was performed using SuperScript III Reverse Transcriptase (Invitrogen, Carlsberg, CA, USA), following the manufacturer's instructions. Real time RT-PCR was performed in duplicate by using Universal SYBR Green Supermix (Bio-Rad) on CFX96 Real Time detection system (Bio-Rad). Relative quantification of gene expression was calculated by the ΔCt (relative expression $\times 10^4$) method. Each Ct value was normalized to the respective *ubiquitin C (UBC)* Ct value. The following primer pairs were used: *TSLPR* forward 5'-ggtagcgttgtctgacactg-3'; *TSLPR* reverse 5'-ttcctgtttggactgccact-3'; *CCL17* forward 5'-tccaggatgccatcgaaaa-3'; *CCL17* reverse 5'-tccctcaactgtggctttct-3'; *TSLPR* reverse ; *GAS6* forward 5'-ctctctgtggcactggtag -3'; *GAS6* reverse 5'-tatgtccacggccagga -3' ; *ALOX15B* forward 5'-ctgagcaaggaggctggaga -3'; *ALOX15B* reverse 5'-gctcatccgataggtgcc-3'; *FCGR2B* forward 5'actgagagtgactggcgtga-t-3'; *FCGR2B* reverse 5'-cacagctgtccacagaagca -3'; *LAIR1* forward 5'-ccgtcgacaacagtacaaa-3'; *LAIR1* reverse 5'-aagaccactgagaccccgat-3'; *MYC* forward 5'-attctctgtctccctcgacg -3'; *MYC* reverse 5'-agcctgcctttccaca-3'; *KLF4* forward 5'-agggagaagacactgcgtca-3'; *KLF4* reverse 5'-tcccggcagcggttattc-3'; *PPARG* forward 5'-aaaggcgagggcgatctg -3'; *PPARG* reverse 5'-gatggccacctttgcct-3'; *UBC* forward 5'-ggtcgcagttctgttg -3'; *UBC* reverse 5'-gatggcttaccagtca-3'.

2.8. RNA-sequencing and bioinformatic analysis

The following samples were employed for next generation sequencing experiments: 3 pairs of *TSLPR⁻* and *TSLPR⁺* mono, each pair obtained from a single donor. Next generation sequencing experiments, comprising samples quality control, were performed by Genomix4life S.R.L. (Baronissi, Salerno, Italy). Indexed libraries were prepared from 1 ug/ea purified RNA with TruSeq Stranded mRNA Sample Prep Kit (Illumina) according to the manufacturer's instructions. Libraries were quantified using the Agilent 2100 Bioanalyzer

(Agilent Technologies) and pooled such that each index-tagged sample was present in equimolar amounts, with final concentration of the pooled samples of 2nM. The pooled samples were subject to cluster generation and sequencing using an Illumina HiSeq 2500 System (Illumina) in a 2x100 paired-end format at a final concentration of 8pmol. The raw sequence files generated (.fastq files) underwent quality control analysis using FastQC (<http://www.bioinformatics.babraham.ac.uk/projects/fastqc/>, release 0.10.1). Raw reads were filtered and trimmed based on quality and adapter inclusion using Trimmomatic (release 0.35) (37).

The human genome and gene annotation file (h38.83) were downloaded from EnsEMBL. First, the genome was indexed using STAR (release 2.5.0b) (38). Then, filtered and trimmed reads were aligned on the genome. SAM output files from STAR were converted into BAM, sorted and indexed using the view, sort, index and programs from the SAMtools software collection (release 0.1.19-96b5f2294a) (39).

The gene annotation file has been collapsed into synthetic file using the createSyntheticTranscripts function from the easyRNASeq package (release 2.6.1) (40). This procedure has been performed to avoid counting reads multiple times by collapsing all existing transcripts of a single gene locus into a “synthetic” transcript containing every exon of that gene. The featureCounts program was used to count the number of reads overlapping genes (release 1.5.0-p1) (41). All the genes not showing at least 1 read mapping per million mapped reads (CPM) in at least 2 samples were discarded. The bioconductor edgeR package (release 3.12.0) (42) was used to calculate the differential expression of genes between two conditions. This package measures the significance of the variation in expression levels using the dispersion of the expression levels among sample replicates. According to the comparison, significantly up/downregulated genes were sorted based on the *p* value. The top 500 differentially expressed genes (DEGs) ($p \leq 0.05$) were used to perform Gene Ontology (GO) enrichment analysis using DAVID tool (release 6.7) (43). Their expression levels were represented in the heatmap using MeV software (multi-experiment viewer – v4.8.1) (44).

2.9. Accession number

The accession number for the RNA sequencing (RNA-seq) data is ArrayExpress: E-MTAB-4996 (<http://www.ebi.ac.uk/ena>).

2.10. Statistical analysis

Statistical analysis was performed with Prism 6 (GraphPad Software). *p* values were calculated with two-tailed paired *t* test, repeated measure one-way or two-way ANOVA corrected for multiple comparisons, or Wilcoxon matched-pairs signed rank test as indicated in figure legends. *p* < 0.05 was considered significant.

3. Results

3.1 TSLP enhances human monocyte production of CCL17

We have recently shown that the STAT5-activating cytokines IL-3 and GM-CSF synergize with the STAT6-activating cytokine IL-4 to enhance human monocyte production of CCL17⁽¹⁴⁾. Since TSLP also activates STAT5⁽²⁾, we stimulated monocytes with TSLP and IL-4 for 21-24 hours in the absence or presence of LPS, which induces monocyte expression of *TSLPR* and *CD127* mRNAs⁽¹⁰⁾, and assessed the production of CCL17. In the absence of LPS only low levels of CCL17 could be detected. CCL17 production could not be detected when monocytes were stimulated with TSLP in the presence or absence of LPS (which is consistent with the absence of myeloid DCs in our monocyte preparations). Interestingly, the addition of TSLP to LPS and IL-4 significantly enhanced CCL17 production (**Figure 5A**). Comparable results were obtained when monocytes were primed with LPS for 14 hours and then stimulated for 21-24 hours with IL-4 and TSLP in the presence or absence of LPS (**Supplementary Figure 1A**). To better characterize the effects of TSLP on monocyte activation, we evaluated the production of TNF- α , IL-1 β , IL-6 and IL-10 upon stimulation with IL-4 and TSLP in the presence of LPS. However, none of these cytokines was significantly modulated by TSLP (**Figure 5B**). Thus, human monocyte activation with TSLP specifically enhances IL-4-induced CCL17 production in the presence of LPS.

3.2. TLR4 activation elicits a subset of human TSLPR⁺ monocytes that preferentially originates from CD16⁻ monocytes

Since TSLP is able to modulate monocyte production of CCL17, we then looked for the surface expression of TSLP receptor complex subunits (TSLPR and CD127) by flow cytometry. Freshly isolated monocytes did not express TSLPR and CD127, nor did they phosphorylate STAT5 in response to TSLP (data not shown). Critically, stimulation of monocytes for 14 hours with LPS induced the expression of TSLP receptor complex subunits on a small percentage of monocytes (TSLPR⁺ mono), while the vast majority expressed only CD127 without TSLPR or neither of them (TSLPR⁻ mono) (**Figure 6A**). We confirmed by imaging cytometry that TSLPR and CD127 co-localize on the surface of TSLPR⁺ mono (**Figure 6C**). Accordingly, when monocytes were pre-treated with LPS and then stimulated with TSLP for 15 minutes, a comparable percentage of monocytes phosphorylated STAT5

(pSTAT5⁺ cells) (**Figure 6B**), indicating that LPS pre-treatment induced the expression of a functional TSLP receptor complex only on a small subset of monocytes.

Next, we sought to characterize whether TLR agonists other than LPS (which is a TLR4 agonist) elicit TSLPR⁺ mono. To this aim, monocytes were pre-treated with LPS (TLR4 agonist), P3CSK4 (TLR2 agonist), Poly(I:C) (TLR3 agonist), flagellin (TLR5 agonist), imiquimod (TLR7 agonist) or ODN 2006 (TLR9 agonist), and then we assessed the expression of TSLPR and CD127 or pSTAT5 in response to TSLP. TLR4 activation induced the highest percentage of TSLPR⁺ mono (**Figure 6D**), although higher concentrations of the TLR2 agonist P3CSK4 also induced TSLPR⁺ mono (**Supplementary Figure 1B**). Interestingly, TSLPR⁺ mono were also elicited by heat-killed Gram-negative bacteria (*Pseudomonas aeruginosa* [HKPA] and *Escherichia coli* O111:B4 [HKEB]), while the heat-killed Gram-positive bacterium *Staphylococcus aureus* (HKSA) had a negligible effect on TSLPR and CD127 surface expression (**Figure 6E**).

Human monocytes can be divided into classical, intermediate and non-classical monocytes based on their expression of CD14 and CD16 (CD14^{hi} CD16⁻, CD14⁺ CD16⁺ and CD14^{dim} CD16⁺, respectively)⁽⁴⁵⁾, although other markers have been proposed to distinguish these subsets⁽⁴⁶⁾. The majority of monocytes in our preparations (which were isolated based on CD14 expression) had a CD14^{hi} CD16⁻ phenotype (classical monocytes), while only a small percentage had a CD14⁺ CD16⁺ phenotype (intermediate monocytes) and virtually no CD14^{dim} CD16⁺ (non-classical) monocytes (**Supplementary Figure 1C, left panel**). To assess the ontogeny of TSLPR⁺ mono, we FACS-sorted CD14^{hi} CD16⁻ and CD14⁺ CD16⁺ monocytes and stimulated them with LPS before assessing TSLPR surface expression. Only a small percentage of CD14⁺ CD16⁺ monocytes became TSLPR⁺ (**Supplementary Figure 1C, right panel**). Since most of the monocytes in our preparations were CD16⁻, it is likely that TSLPR⁺ mono preferentially originated from this subset with a rather minor contribution of CD14⁺ CD16⁺ monocytes.

3.3. TLR4-activated signaling pathways required for the induction of TSLPR⁺ monocytes

Pro-inflammatory and infectious stimuli induce the expression of TSLP receptor complex as well as its ligand TSLP in epithelial cells⁽⁴⁷⁻⁴⁹⁾. However, the expression of TSLP receptor

complex in this model is not mediated by nuclear factor NF- κ B, since overexpression of the NF- κ B subunits p50 and p65 does not induce TSLP receptor complex, nor does the inhibitor BAY 11-7082 (which inhibits TNF- α -induced I κ B α phosphorylation and thus NF- κ B nuclear translocation) impair its expression. On the contrary, both approaches affect TSLP expression (48). To evaluate the contribution of NF- κ B to the expression of TSLP receptor complex in our model, we stimulated monocytes with LPS in the presence of different concentrations of BAY 11-7082. Interestingly, BAY 11-7082 concentration-dependently reduced the percentage of TSLPR $^+$ mono (**Figure 7A**). Since TNF- α induces TSLP receptor complex expression in epithelial cells and human hematopoietic progenitors (47, 50), we also evaluated the contribution of LPS-induced autocrine TNF- α to TSLP receptor expression. The addition of an anti-TNF- α blocking antibody to LPS did not significantly modify the percentage of TSLPR $^+$ mono (**Supplementary Figure 2A**), thus ruling out any role for TNF- α in our model. TLR4 also signals through MAPKs (i.e. ERK1/2, p38, JNK) (51), which may be involved in the modulation of TSLP receptor complex. Indeed, the p38 inhibitor SB203580 reduced (**Figure 7B**), while inhibitors of MEK1/2 (U0126, which in turn inhibits ERK1/2) and JNK (SP600125) had no effect on the percentage of TSLPR $^+$ mono (**Supplementary Figure 2B**).

LPS-mediated TLR4 activation triggers the PI3K/Akt pathway, which exerts anti-inflammatory properties at least in part by restraining NF- κ B and GSK-3 pro-inflammatory activities (51). Since the TLR4-mediated monocyte pro-inflammatory activation is required for eliciting TSLPR $^+$ mono, we evaluated the role of PI3K in our model. The PI3K inhibitors wortmannin and LY294002 markedly increased the percentage of TSLPR $^+$ mono. To test the balance between PI3K and GSK-3, we employed the GSK-3 inhibitor CHIR-98014. Interestingly, CHIR-98014 alone did not modulate the percentage of TSLPR $^+$ mono. However, when CHIR-98014 was administered along with the PI3K inhibitors it completely reverted their effect, since the percentage of TSLPR $^+$ mono in these conditions was comparable to that of monocytes stimulated with LPS without any inhibitors (**Figure 7C**).

3.4. TSLPR $^+$ monocytes exhibit discrete phenotypic and functional features

The results obtained so far support a model in which the balance between intracellular pro-inflammatory (e.g. NF- κ B, p38, GSK-3) and anti-inflammatory (e.g. PI3K) pathways activated by LPS dictates the emergence of TSLPR $^+$ mono. We next decided to characterize the phenotypic and functional features of TSLPR $^+$ and TSLPR $^-$ mono. First, we evaluated the

surface expression of the myeloid cell markers CD14, CD11b and CD11c. Although they were expressed by both subsets, TSLPR⁺ mono exhibited higher levels of CD11c, and lower levels of CD14 and CD11b (**Supplementary Figure 2C**). Then, we assessed the response of TSLPR⁺ and TSLPR⁻ mono to LPS, IL-4 and TSLP. Monocytes were pre-treated for 14 hours with LPS, FACS-sorted into TSLPR⁺ and TSLPR⁻ mono and stimulated for 16-18 hours in the presence of LPS without or with IL-4, TSLP or a combination of them. Interestingly, *TSLPR* mRNA was expressed by TSLPR⁺ mono while it was not induced in TSLPR⁻ mono under any of the tested conditions (**Figure 8A**), suggesting that once the distinction between these subsets is established during LPS pre-treatment it remains stable. We also assessed *CCL17* mRNA levels and surprisingly we found that only TSLPR⁺ mono expressed *CCL17* in response to IL-4 (**Figure 8B**), despite both subsets phosphorylated STAT6 in response to IL-4 (data not shown) and TSLPR⁺ mono did not express higher levels of transcription factors involved in monocyte/macrophage alternative activation (i.e. *MYC*, *KLF4*, *PPARG*) (**Supplementary Figure 2D**)⁽⁵²⁻⁵⁵⁾. These results were confirmed by evaluating CCL17 protein levels in cell-free supernatants (**Figure 8C**). To account for possible cross-talks between TSLPR⁺ mono and TSLPR⁻ mono that could result in the expression of CCL17 also in the TSLPR⁻ subset, monocytes were pre-treated with LPS and IL-4 and FACS-sorted TSLPR⁺ and TSLPR⁻ mono were directly harvested for RNA isolation without further re-stimulation. In keeping with our previous results, the expression of *TSLPR* and *CCL17* mRNAs was higher in the TSLPR⁺ subset (**Figure 8D**). To further characterize the response of TSLPR⁺ and TSLPR⁻ mono we evaluated the production of TNF- α , IL-1 β , IL-6 and IL-10, and found that in each of the tested conditions TSLPR⁺ mono produced respectively lower and higher levels of IL-6 and IL-10. TSLPR⁺ mono showed reduced TNF- α production only when stimulated with LPS and TSLP, while no significant differences in the production of IL-1 β were observed (**Figure 8E**).

These results support the concept of an LPS-induced functional specialization in an apparently homogeneous population of human CD14⁺ monocytes. To gain further insights into this model, we performed a transcriptomic analysis of FACS-sorted TSLPR⁺ and TSLPR⁻ mono re-stimulated with LPS for 14 hours. Gene ontology (GO) analysis revealed distinct enrichment for biological processes between TSLPR⁻ and TSLPR⁺ mono (**Figure 9A, 9B**). Moreover, these cell subsets also exhibited different gene expression profiles (**Figure 10**). Unexpectedly, TSLPR⁺ mono expressed higher levels of *CD1C*, a marker of DCs^(56, 57) assigned to the conventional DC 2 (cDC2) lineage⁽⁵⁸⁾, and also of genes that are commonly

associated with antigen processing and presentation (e.g. *LAMP3*, MHC class II genes) (**Supplementary Tables I, II**). These results are consistent with the increased surface expression of HLA-DR (**Figure 11A**). We also confirmed the surface expression of CD1c in TSLPR⁺ mono, while it was not expressed by TSLPR⁻ mono (**Figure 11B**). Since one of the main features of DCs is antigen presentation and the ability to induce T cell proliferation, we challenged TSLPR⁺ and TSLPR⁻ mono (re-stimulated for 14 hours with LPS or LPS and IL-4) with CFSE-labeled CD4⁺ T lymphocytes isolated from an unrelated donor. TSLPR⁺ mono re-stimulated with LPS were the most efficient in promoting T cell proliferation, although the overall proliferation rate was low and consistent with the monocytic origin of these cells (**Figure 11C**). GO analysis also revealed enrichment for genes associated with cell motility in TSLPR⁺ mono (**Figure 9B**). To corroborate these findings, we performed time-lapse microscopy of TSLPR⁺ and TSLPR⁻ mono re-stimulated as indicated above. TSLPR⁺ mono displayed increased cell motility and mean square displacement (MSD) (**Figure 11D**) in cell tracking experiments. Finally, we confirmed that TSLPR⁺ mono re-stimulated with LPS or LPS and IL-4 expressed higher levels of genes with important immune functions (**Figure 12**): *GAS6*, ligand of the TAM receptor AXL that exerts several functions including promoting tumor growth⁽⁵⁹⁾; *ALOX15B*, an enzyme involved in the synthesis of pro-resolving lipid mediators⁽⁶⁰⁾; *FCGR2B* and *LAIR1*, inhibitory receptors that bind respectively the constant region of IgG and collagen or collagen-like motif-containing proteins (e.g. C1q and surfactant protein D)^(61, 62).

3.5. TSLPR is preferentially expressed by a subset of CD14⁺ CD1c⁺ monocytes

The evidence of increased CD1c expression among TSLPR⁺ mono was rather unexpected since CD1c is commonly considered a surface marker of cDC2^(56, 57). Thus, we decided to investigate the expression of CD1c in our preparations of CD14⁺ monocytes by flow cytometry. Surprisingly, we found that approximately 1% of monocytes in our preparations exhibited a CD14⁺ CD1c⁺ phenotype. Comparable results were obtained with LPS-stimulated monocytes (**Figure 13A**). Of note, the majority of CD14⁺ CD1c⁺ monocytes expressed TSLPR upon LPS stimulation, although TSLPR was also expressed by a small percentage of CD14⁺ CD1c⁻ that may significantly contribute to the population TSLPR⁺ mono owing to the high number of CD14⁺ CD1c⁻ cells in our preparations (**Figure 13B**). Nevertheless, LPS-

stimulated CD14⁺ CD1c⁺ monocytes expressed the highest levels of TSLPR as assessed on total CD14⁺ CD1c⁺ (**Figure 13C, 13D**) or CD14⁺ CD1c⁺ TSLPR⁺ cells (**Figure 13E**).

3.6. In vivo monocyte expression of TSLPR and CD127 in Gram-negative sepsis

So far we have characterized the signals that elicit TSLPR⁺ mono and the phenotypic and functional properties of this subset *in vitro*. To evaluate the *in vivo* relevance of our findings, we took advantage of public available microarray (GSE46955) performed on human CD14⁺ monocytes isolated from patients with a diagnosis of Gram-negative sepsis (blood culture positive for *Escherichia coli*) and after their complete recovery (i.e. 1-3 months after resolution), as well as healthy control⁽⁶³⁾. By analysing these data we found that monocytes isolated from patients with Gram-negative sepsis expressed increased levels of *TSLPR* and *CD127* mRNAs compared to healthy controls (**Figure 14A**). Interestingly, expression levels of both genes were reduced after recovery (**Figure 14B**), likely linking monocyte expression of TSLP receptor complex to TLR4 activation *in vivo*.

4. Discussion

The starting point of our investigation was the responsiveness of human CD14⁺ monocytes to TSLP. Although we demonstrate that TSLP modulates CCL17 production, we have not fully characterized its effects on human monocytes, nor have we identified a specific response elicited by TSLP alone in the absence of IL-4. Instead, we decided to focus our attention on the characterization of TSLPR⁺ mono, which was an unexpected yet interesting aspect of our study. The identification of TSLPR⁺ mono may also contribute to a deeper understanding of human monocyte responsiveness to TSLP, since it raises the question of whether TSLPR⁺ mono are the sole monocyte subset that can be activated by TSLP. Even more importantly, LPS induces TSLPR expression on the majority of CD14⁺ monocytes that co-expresses the myeloid DC marker CD1c. TSLPR expression on this subset of CD14⁺ CD1c⁺ monocytes is higher compared to CD14⁺ CD1c⁻ cells. Thus, the population of TSLPR⁺ mono is composed of CD14⁺ CD1c⁺ and CD14⁺ CD1c⁻ monocytes, and it is tempting to speculate that some if not most of the properties we have identified for TSLPR⁺ mono may actually be ascribed to CD14⁺ CD1c⁺ cells. Nevertheless, the percentage of TSLPR⁺ mono is not only reduced by NF-κB and p38 inhibitors, but is also increased by PI3K inhibitors via activation of GSK-3. These results highlight a complex network of intracellular pathways that regulates TSLPR expression and also argue against the hypothesis that TSLPR⁺ mono derive solely from pre-committed precursors. Indeed, it would be unlikely to increase the percentage of TSLPR⁺ mono using PI3K inhibitors if this subset originated exclusively from pre-committed precursors. It is conceivable that TSLPR⁺ mono also emerge from LPS-stimulated CD14⁺ CD1c⁻ monocytes through a stochastic process dictated by the intracellular balance between pro-inflammatory (e.g. NF-κB, p38, GSK-3) and anti-inflammatory (e.g. PI3K) pathways. Once this intracellular balance has been established, it is likely to influence subsequent responses of TSLPR⁺ and TSLPR⁻ mono. For example, re-stimulation of TSLPR⁻ mono does not induce *TSLPR* expression. Moreover, it would be interesting to evaluate whether such modulation of signaling pathways also promotes the conversion of CD14⁺ CD1c⁻ toward CD14⁺ CD1c⁺ monocytes. Interestingly, studies performed at the single cell level have revealed, in contrast to population-level studies, a remarkable heterogeneity in the activation of signaling pathways and gene expression programs upon stimulation of apparently homogeneous populations⁽⁶⁵⁻⁶⁶⁾. Moreover, it is now clear that even innate immune cells preserve memory of their previous stimulation^(67, 68). Further studies are required to understand the relative contribution of pre-committed CD14⁺ CD1c⁺ progenitors and their

relationship to CD14⁺ CD1c⁻ monocytes as well as stochastic differences in the activation of signaling pathways to the emergence of TSLPR⁺ mono.

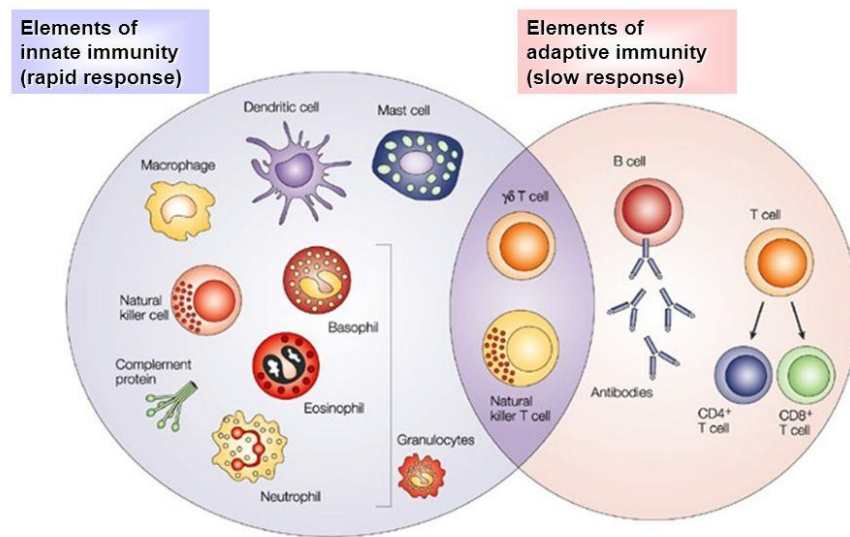
The existence of CD14⁺ CD1c⁺ cells (referred to as human inflammatory DCs, infDCs) has been reported in several inflammatory conditions, including ovarian and breast tumor ascites⁽⁶⁹⁾. infDCs induce higher CD4⁺ T cell proliferation and Th17 skewing compared to CD14⁺ CD16⁺ CD1c⁻ inflammatory macrophages isolated from the same tissue, probably due to their ability to produce the Th17-polarizing cytokine IL-23⁽⁷⁰⁾. While this manuscript was in preparation, the presence of CD14⁺ CD1c⁺ monocytes has been reported in the peripheral blood of healthy donors and mucosal tissues isolated from distal duodenum/proximal jejunum of pancreatic cancer patients, nasal mucosa of healthy donors or allergic patients, or bronchial mucosa obtained from patients with non-small cell lung carcinoma⁽⁷¹⁾. Importantly, the frequency of this subset is elevated in the peripheral blood of stage III or IV melanoma patients and in skin melanoma lesions compared to healthy donors⁽⁷²⁾. CD14⁺ CD1c⁺ cells are less efficient at inducing CD4⁺ T cell proliferation compared to CD1c⁺ DCs (suggesting their classification as monocytes)^(71, 72) and also exhibit a unique gene signature⁽⁷²⁾. We demonstrate that CD14⁺ CD1c⁺ cells express higher levels of TSLPR in response to LPS compared to CD14⁺ CD1c⁻ monocytes. Interestingly, TSLP promotes myeloid DC maturation, cytokine production and their ability to induce CD4⁺ T cell proliferation and polarization toward distinct phenotypes (e.g. Th1, Th2, Th17) depending on the inflammatory milieu. It will be interesting to evaluate whether TSLP exerts similar effects on CD14⁺ CD1c⁺ cells. Indeed, it is likely that this monocyte subset is the most responsive to TSLP. Further studies are warranted to assess the spectrum of responses elicited by TSLP in CD14⁺ CD1c⁺ TSLPR⁺ cells.

Among the list of differentially expressed genes we confirmed that TSLPR⁺ mono express higher levels of gene with important immune-related functions: *GAS6*, *ALOX15B*, *FCGR2B* and *LAIR1*. *GAS6* encodes the vitamin K-dependent protein GAS-6 that is mainly produced by endothelial cells, vascular smooth muscle cells and hematopoietic cells. It binds the TAM receptor tyrosine kinases, especially AXL, and as such is involved in the regulation of inflammation, promotes tissue repair and vascular homeostasis, and modulates both cancer cell growth and tumor-associated immune cell functions⁽⁵⁹⁾. Of note, tumor cells promote GAS-6 production by tumor-associated macrophages that in turn promote cancer growth and metastasis⁽⁷³⁾. *ALOX15B* encodes the enzyme arachidonate 15-lipoxygenase B (15-LOX-B) that mainly catalyzes the conversion of arachidonate into 15(S)-HpETE, which is in turned

converted to 15(S)-HETE that acts as a precursor for the synthesis of the pro-resolving lipid mediators lipoxins⁽⁶⁰⁾. *FCGR2B* encodes the only receptor (Fc γ RIIB) for the constant region of IgG endowed with inhibitory properties⁽⁶¹⁾. *LAIR1* encodes an inhibitory receptor (LAIR-1 or CD305) for collagen or collagen-like motif-containing proteins (e.g. C1q and surfactant protein D). Its activation impairs monocyte cytokine production and differentiation toward DCs^(62, 74-76). Considering these results with the increased production of CCL17 and IL-10 and the lower production of IL-6 by TSLPR⁺ mono, it is tempting to speculate that this subset is endowed with immunoregulatory/anti-inflammatory properties. Again, whether these properties belong to CD14⁺ CD1c⁺ TSLPR⁺ cells, CD14⁺ CD1c⁻ TSLPR⁺ cells or both subsets remains to be established.

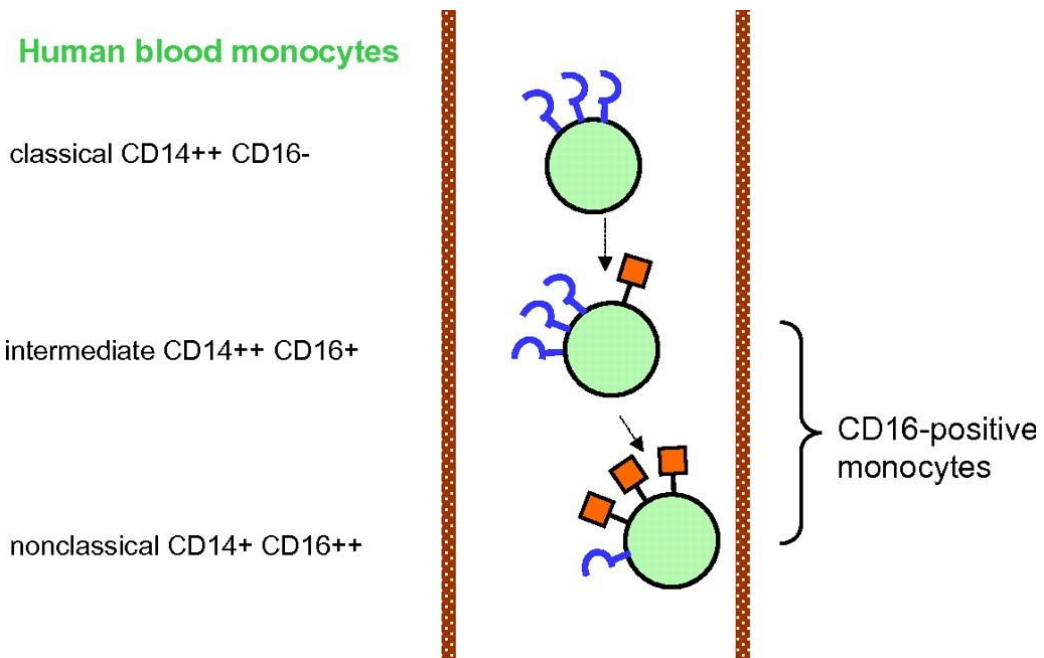
In conclusion, by investigating human CD14⁺ monocyte responsiveness to TSLP we unravel a previously unknown phenotypic and functional heterogeneity marked by differential TSLPR expression. The expression of the myeloid DC marker CD1c within the TSLPR⁺ mono subset revealed further heterogeneity. Indeed, peripheral blood monocytes can be divided into CD14⁺ CD1c⁻ and CD14⁺ CD1c⁺ cells, the latter expressing the highest levels of TSLPR upon LPS stimulation. Considering the increased expression of *TSLPR* mRNA in CD14⁺ monocyte isolated from patients with Gram-negative sepsis, the expansion of CD14⁺ CD1c⁺ cells in the peripheral blood of melanoma patients and their unique gene expression signature, further efforts should be made to characterize the functional properties of this subset (e.g. responsiveness to TSLP), its relationship to CD14⁺ CD1c⁻ monocytes and cDC2 as well as its relevance *in vivo*.

5. Figure legends



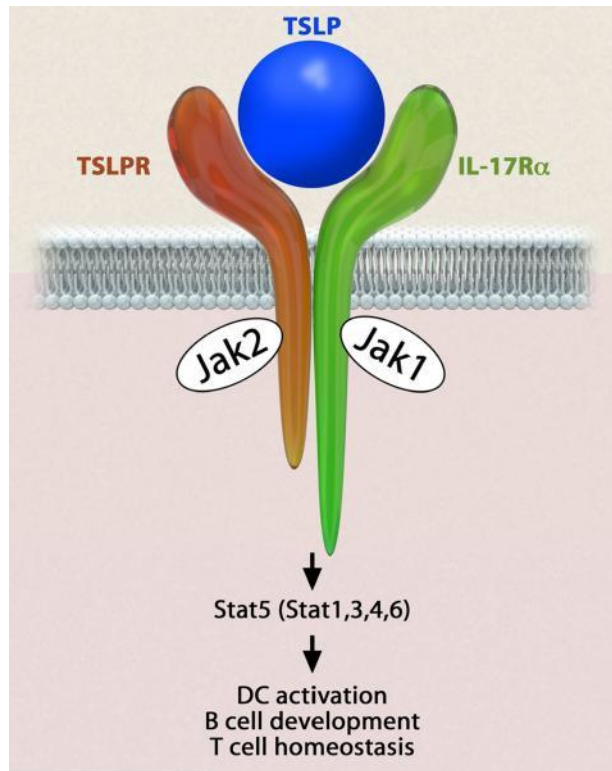
From Dranoff G. 2004. *Nature Reviews Cancer*. 4: 11-22

Figure 1. The innate immune response functions as the first line of defence against infection. It consists of soluble factors, such as complement proteins, and diverse cellular components including granulocytes (basophils, eosinophils and neutrophils), mast cells, macrophages, dendritic cells and natural killer cells. The adaptive immune response is slower to develop, but manifests as increased antigenic specificity and memory. It consists of antibodies, B cells, and CD4⁺ and CD8⁺ T lymphocytes. Natural killer T cells and $\gamma\delta$ T cells are cytotoxic lymphocytes that straddle the interface of innate and adaptive immunity ⁽²¹⁾.



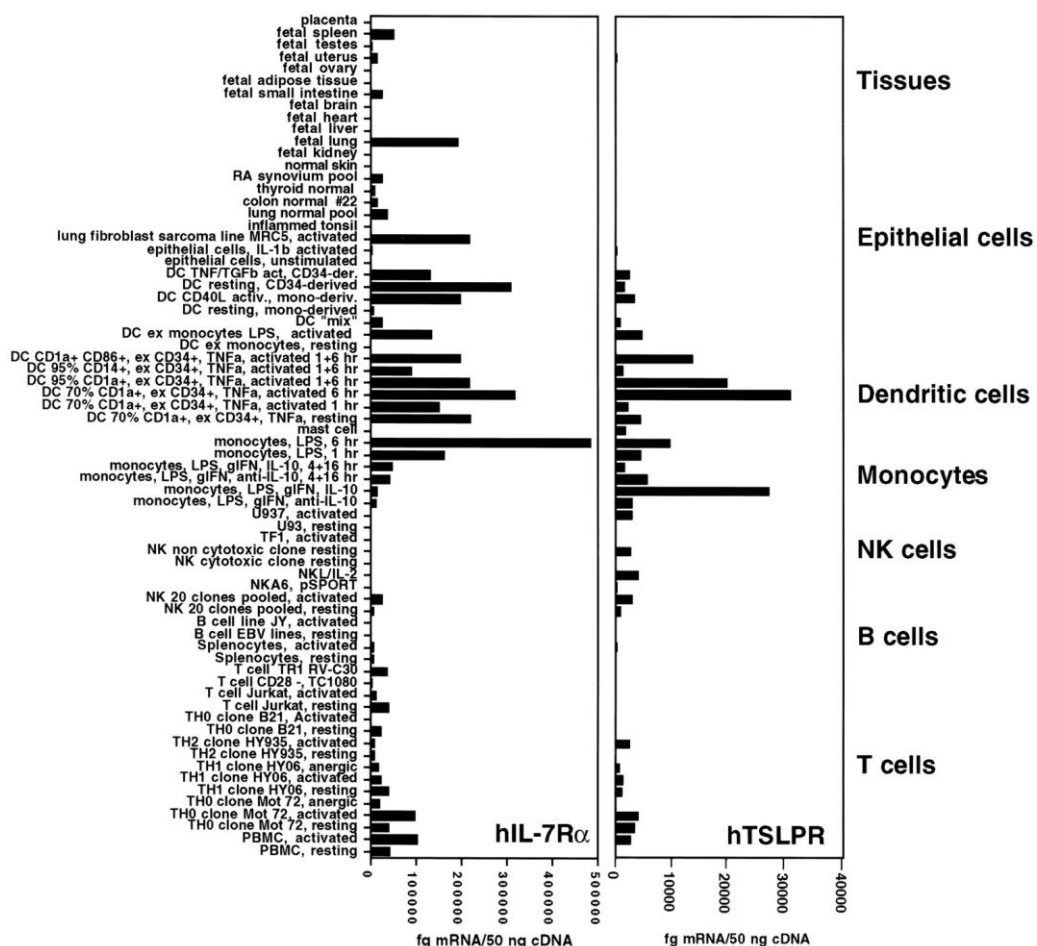
Adapted from Ziegler-Heitbrock L. 2010 Blood 116: 74-80

Figure 2. Nomenclature of monocytes and DCs in blood. Blue hook indicates CD14; red square flag, CD16⁽⁷⁷⁾.



From Ziegler SF 2012 J Allergy Clin Immunol 130: 845-52

Figure 3. Schematic representation of the TSLP receptor complex. Schematic of TSLP bound by the TSLP receptor. JAK1 and JAK2, as well as the STAT proteins shown to be activated following receptor engagement, are indicated. STAT5 is in bold as it is the predominant STAT protein that is activated⁽⁷⁸⁾.



From Reche P. A. 2001 *The Journal of Immunology* 67: 336-343

Figure 4. Expression profiles of TSLPR and IL-7Ra. Expression of TSLPR and IL-7Ra was measured by quantitative PCR on a panel of human (h) cDNA libraries made from various tissues and cell types. Cells were often left untreated or were treated with different stimuli as indicated before RNA was isolated. Expression levels were normalized and expressed as femtograms per 50 ng total cDNA. Coexpression of TSLPR and IL-7Ra was detected in DC, monocytes, and, to a lesser extent, T cells (10).

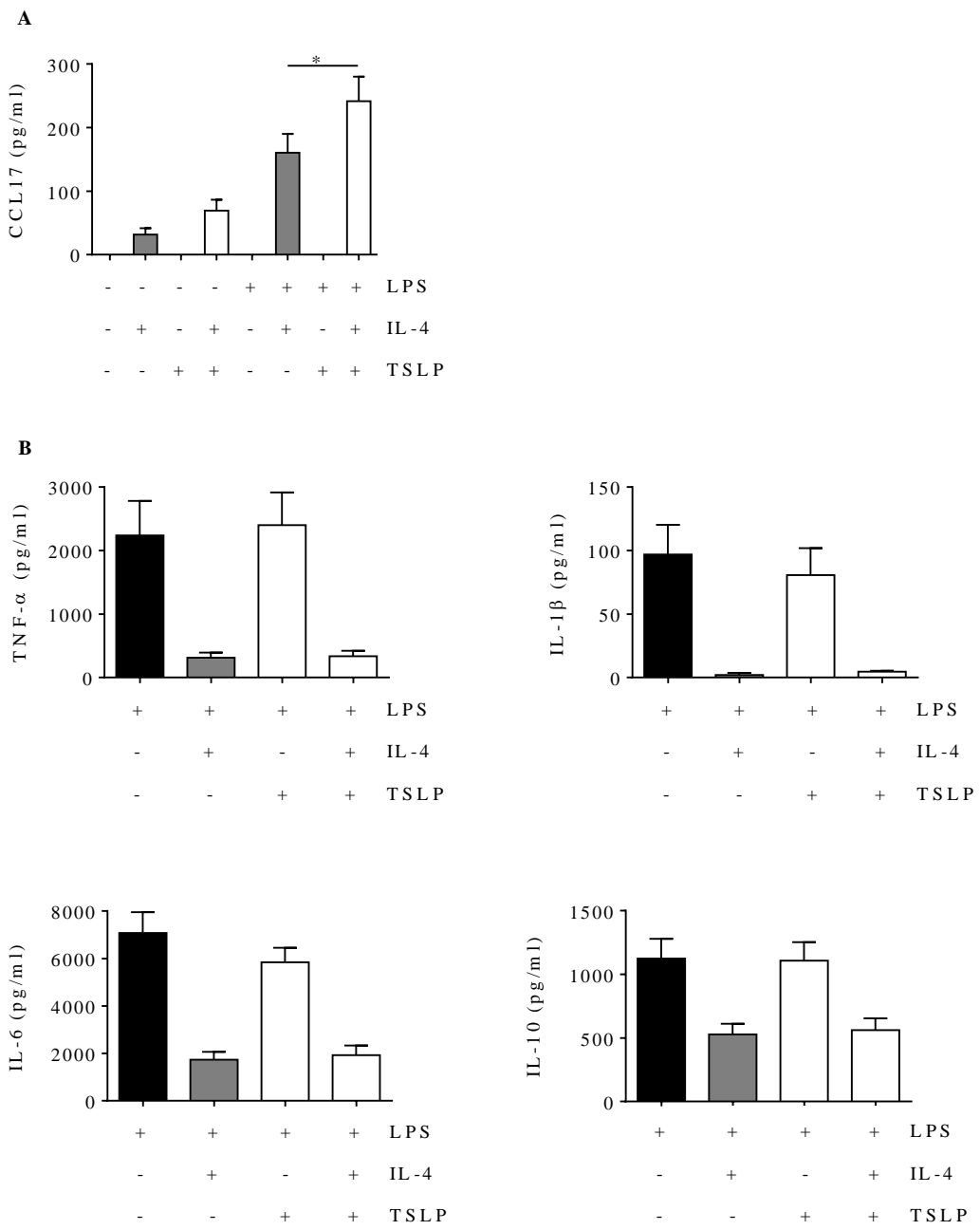


Figure 5. TSLP enhances LPS and IL-4-induced CCL17 production (A and B). Human CD14+ monocytes were stimulated with IL-4 and TSLP in the absence or presence of LPS for 21-24 hours. CCL17, TNF- α , IL-1 β , IL-6 and IL-10 levels were assessed by ELISA in cell-free supernatants. Data are shown as mean + SEM of 11 (A) or 8 (B) independent experiments. * p < 0.05 determined by repeated measure one-way ANOVA with Tukey's post hoc test.

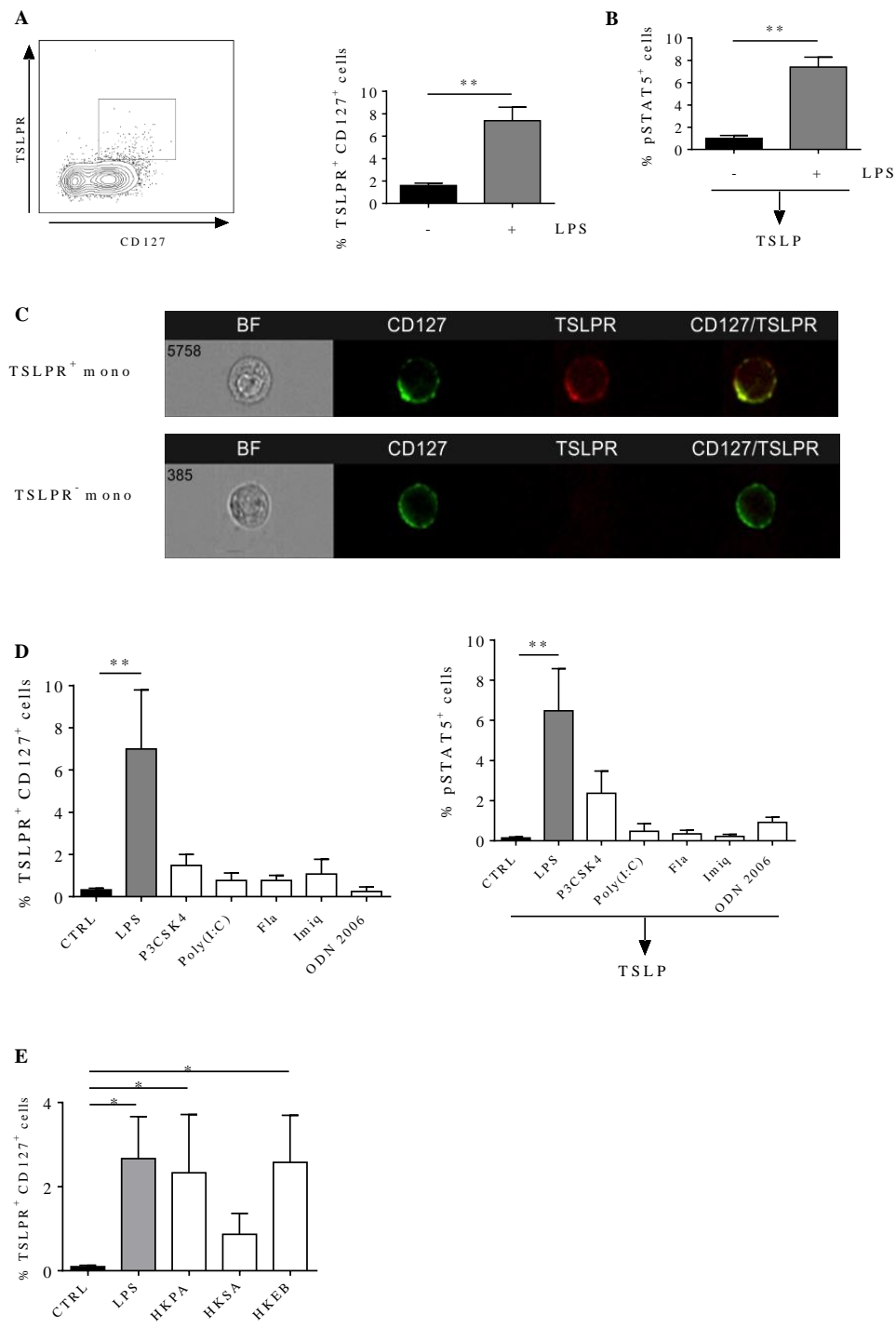


Figure 6. LPS stimulation elicits a subset of TSLPR+-expressing monocytes (TSLPR+ mono). (A, B, D, E) Human CD14+ monocytes were stimulated with LPS (A, B), several TLR agonists (D) or heat-killed bacteria (E) for 14 hours and the percentages of TSLPR+ CD127+ cells (TSLPR+ mono) (A, D, E) or pSTAT5+ cells in response to TSLP (B, D) were assessed by flow cytometry. A representative contour plot of TSLPR and CD127 expression is shown in A, left panel. (C) Cells were treated as in A and the expression and co-localization of TSLPR and CD127 were assessed in TSLPR+-mono (upper panel) or TSLPR- mono (lower panel) by imaging cytometry. A representative cell for each subset is shown. Data are shown as mean + SEM of 9 (A, B), 4 (D) or 6 (E) independent experiments. * $p < 0.05$, ** $p < 0.01$ determined by two-tailed paired t test (A, B) and repeated measure one-way ANOVA with Dunnett's post hoc test (D, E).

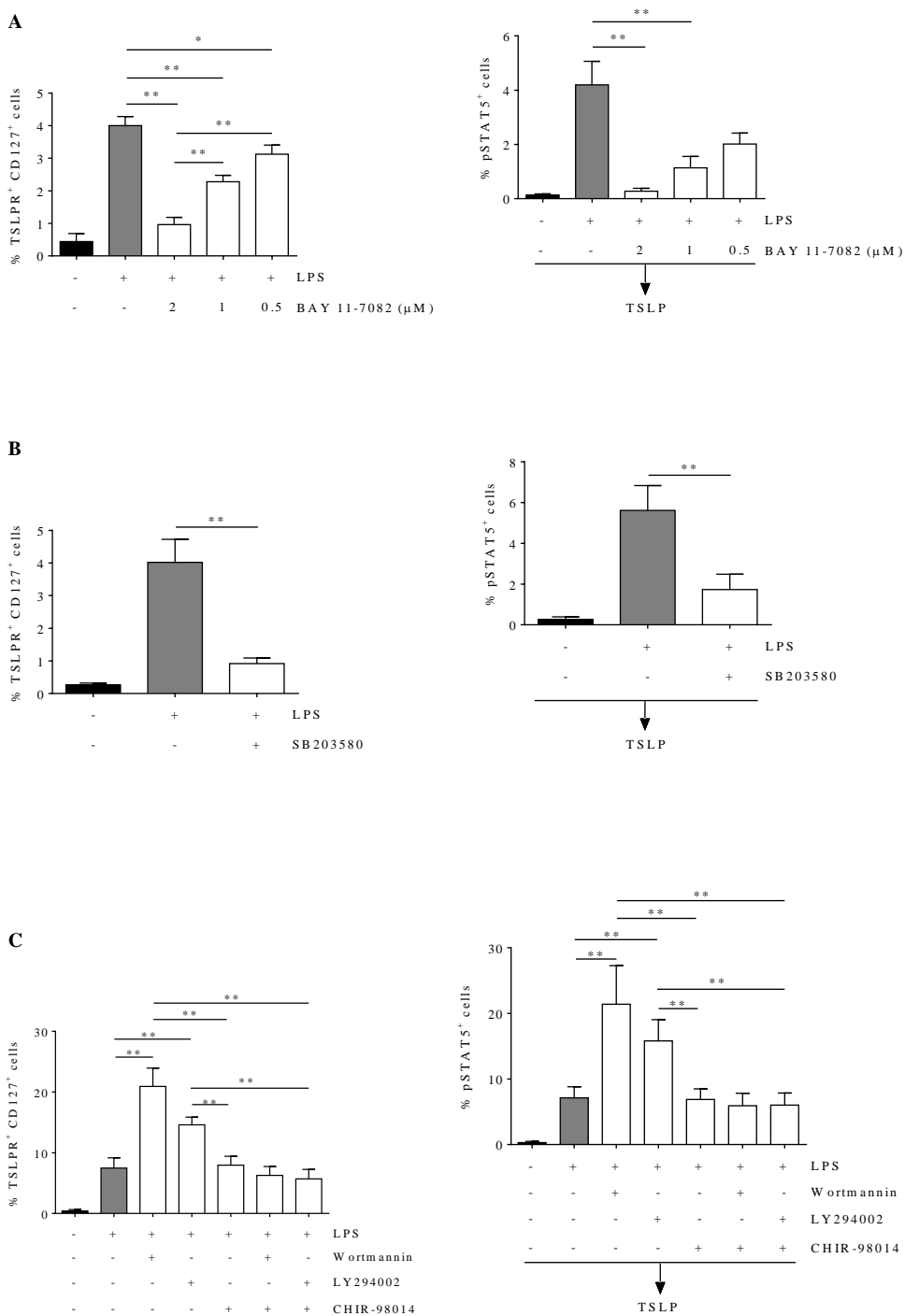


Figure 7. Signaling pathways required for TSLPR+-mono emergence. (A-C) Human CD14+ monocytes were stimulated with LPS in the presence or absence of BAY 11-7082 (NF- κ B inhibitor) (A), SB203580 (p38 inhibitor) (B), wortmannin, LY294002 (PI3K inhibitors) and CHIR-98014 (GSK-3 inhibitor) (C) for 14 hours and the percentages of TSLPR+ CD127+ cells (left panels) or pSTAT5+ cells in response to TSLP (right panels) were assessed by flow cytometry. Data are shown as mean + SEM of 5 (A) or 6 (B, C) independent experiments. * $p < 0.05$, ** $p < 0.01$ determined by repeated measure one-way ANOVA with Tukey's post hoc test.

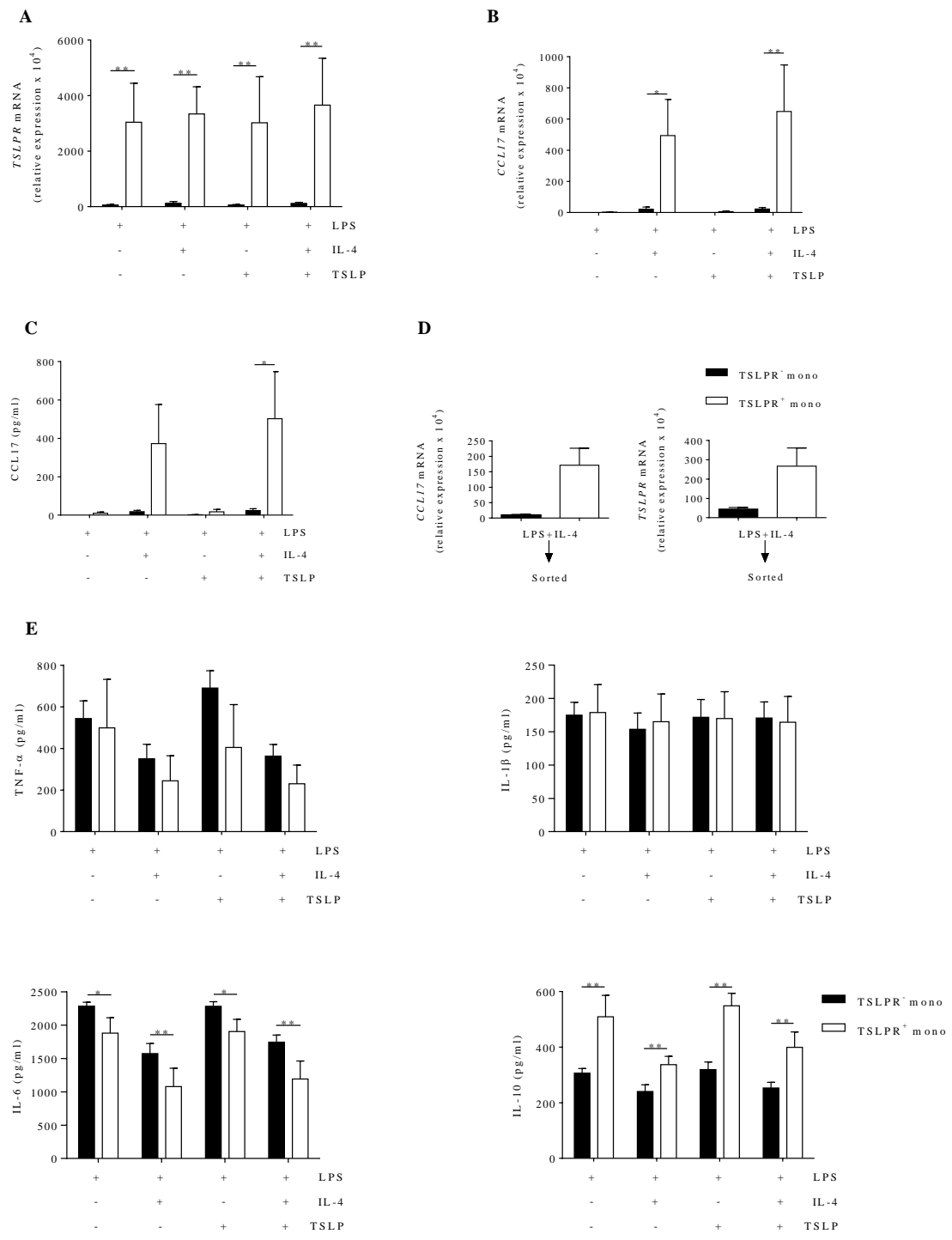


Figure 8. TSLPR⁺ mono display a different cytokine profile. (A-E) Human CD14⁺ monocytes were pre-treated with LPS (A-C, E) or LPS + IL-4 (D) for 14 hours and FACS-sorted into TSLPR⁻ and TSLPR⁺ mono. Then, cells were directly harvested for RNA isolation and real time RT-PCR analysis (D) or further stimulated with LPS, IL-4 and TSLP for 16-18 hours (A-C, E). Cytokine levels were assessed in cell-free supernatants by ELISA (C, E) and cells were harvested for RNA isolation and real time RT-PCR analysis (A, B). Black bars, TSLPR⁻ mono. White bars, TSLPR⁺ mono. Data are shown as mean + SEM of 4 (A-C, E), or 2 (D) independent experiments. * p < 0.05, ** p < 0.01 determined by repeated measure one-way ANOVA with Sidak's post hoc test (A-C, E).

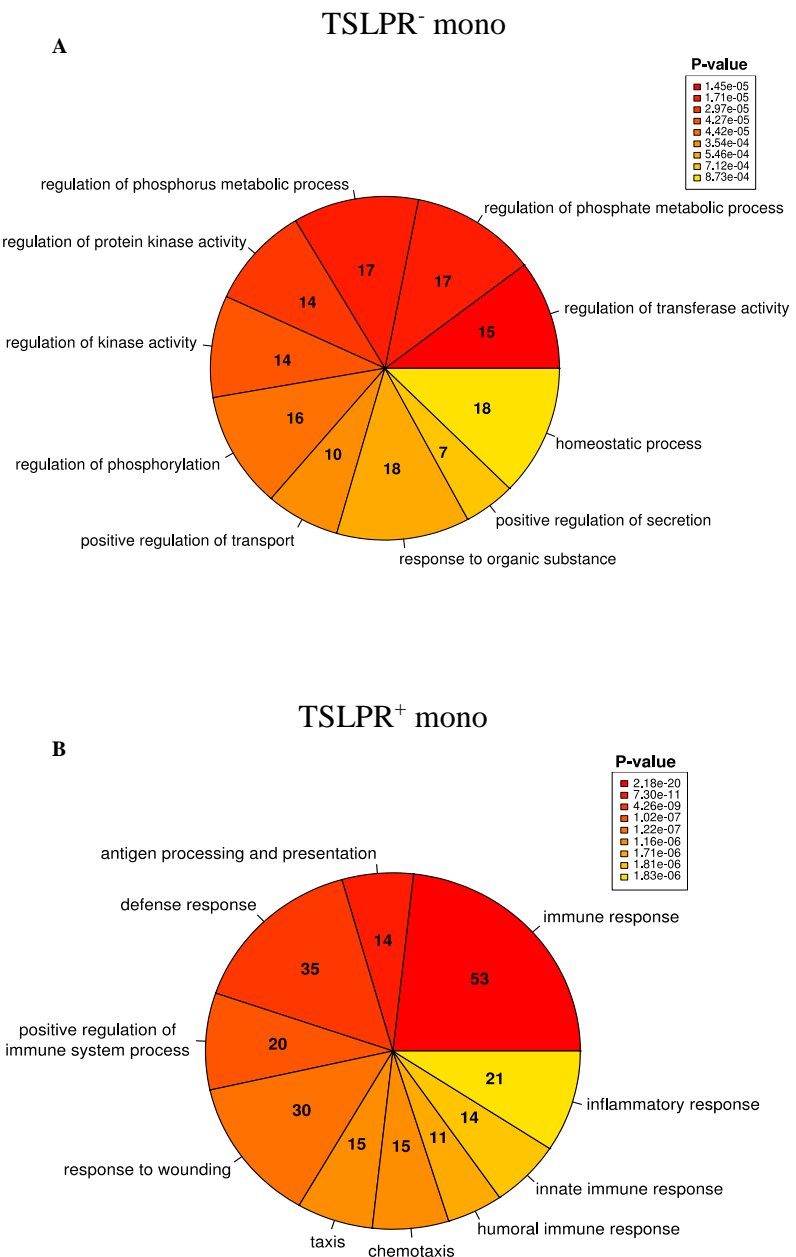


Figure 9. Transcriptomic analysis of TSLPR- and TSLPR+ mono re-stimulated with LPS. (A, B) Pie-charts show the top ten biological functions by the 178 (A) and 322 (B) genes upregulated in TSLPR- and TSLPR+ human monocytes, respectively. The colour gradient indicates the GO terms ordered based on the p value ($p \leq 0.01$, darker colors indicate lower p values).

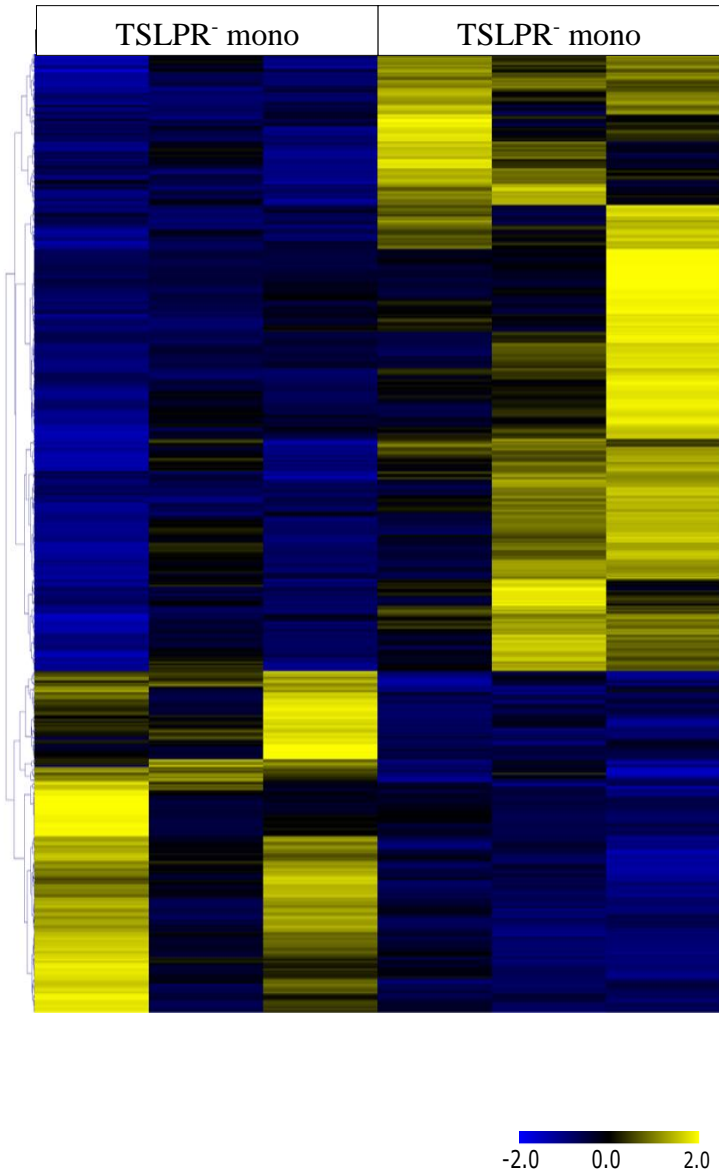


Figure 10. Transcriptomic analysis of TSLPR- and TSLPR+ mono re-stimulated with LPS. Hierarchical clustering of the top 500 genes (rows) based on their relative expression levels in each sample (column). Yellow and blue indicate high and low expression levels, respectively.

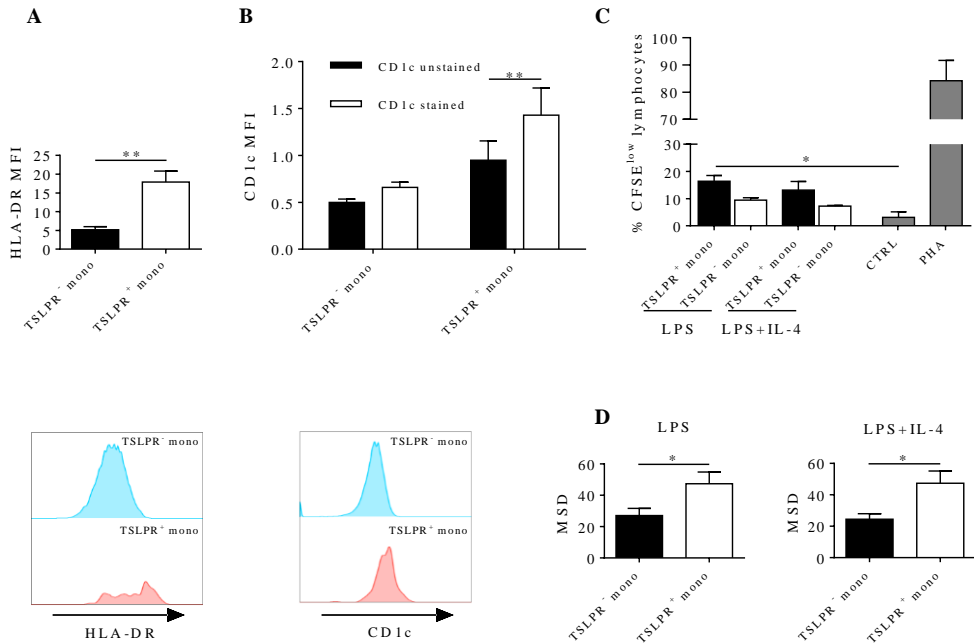


Figure 11. TSLPR⁺ mono exhibit different phenotypic and functional properties. (A, B) Human CD14⁺ monocytes were stimulated with LPS for 14 hours and the expression of (A) HLA-DR and (B) CD1c was assessed by flow cytometry as median fluorescence intensity (MFI). Lower panels, representative histograms of (A) HLA-DR and (B) CD1c expression in TSLPR⁻ and TSLPR⁺ mono. (C) Human CD14⁺ monocytes were pre-treated with LPS for 14 hours and FACS-sorted into TSLPR⁺ and TSLPR⁻ mono. (C) Cells were stimulated with LPS or LPS + IL-4 for 14 hours, washed and then cultured with CFSE-labeled CD4⁺ T lymphocytes isolated from unrelated donors for 7 days. Unstimulated (CTRL) and phytohemagglutinin-stimulated (PHA) lymphocytes were used as controls. The percentage of CFSE^{low} (i.e. proliferating) cells was assessed by flow cytometry. (D) Cells were stimulated with LPS or LPS + IL-4 for 14 hours and digital phase contrast images were taken every 15 minutes with a 20x objective. Cell movements were expressed as mean square displacement (MSD, mean squared distance between cell positions at the end and at the beginning of the cell-tracking experiment). Data are shown as mean + SEM (A-D) of 6 (A, B), 3 (C) or 4 (D) independent experiments. * p < 0.05, ** p < 0.01 determined by two-tailed paired t test (A, D), repeated measure two-way ANOVA with Sidak's post hoc test (B), repeated measure one-way ANOVA with Tukey's post hoc test (C).

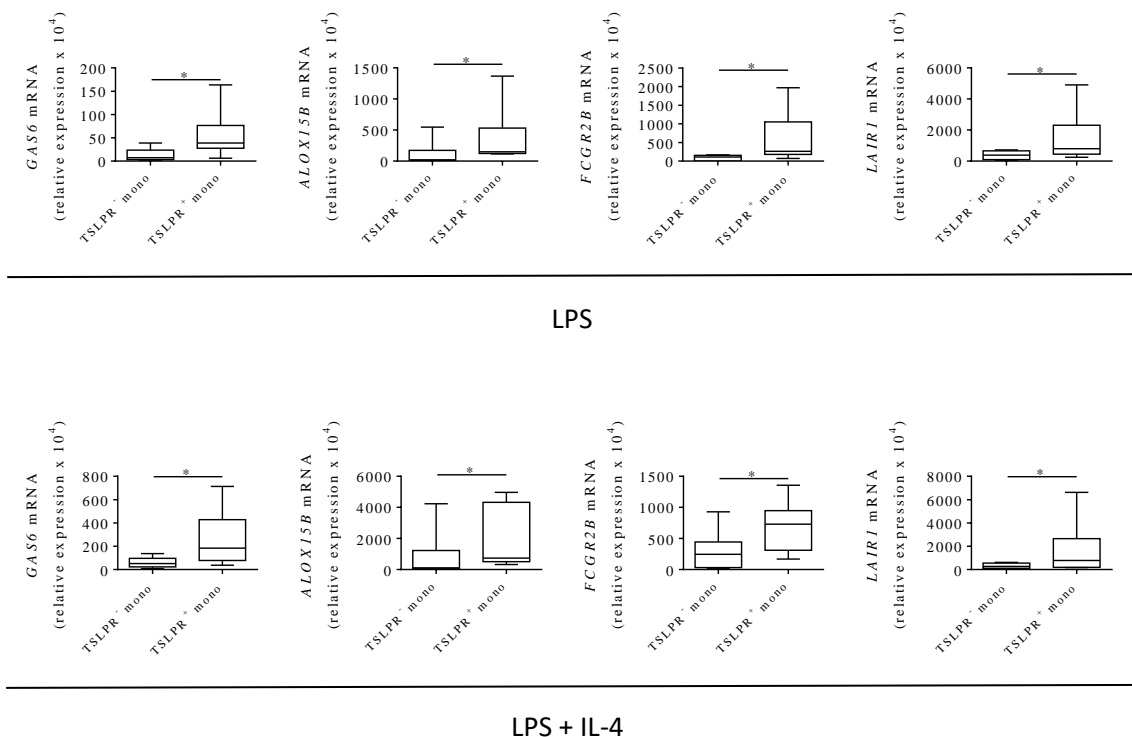


Figure 12. TSLPR+ mono exhibit different phenotypic and functional properties. Cells were stimulated with LPS or LPS+IL-4 for 14 hours and then harvested for RNA isolation and subsequent real time RT-PCR analysis. Data are shown as the median, the 25th and 75th percentiles (boxes) and the 5th and 95th percentiles (whiskers) of 6 independent experiments. * $p < 0.05$ determined by Wilcoxon matched-pairs signed rank test.

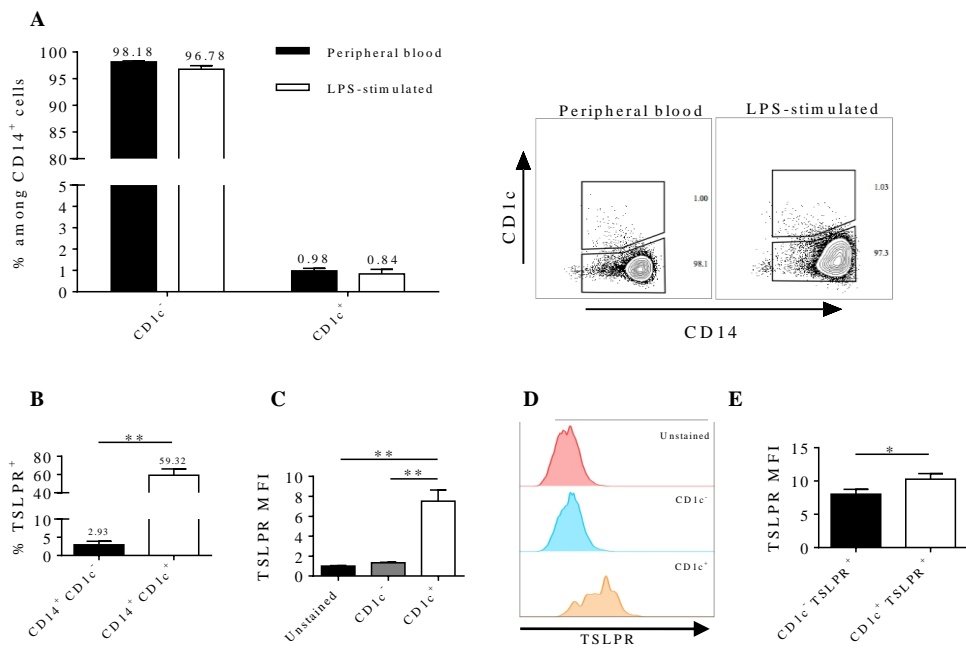


Figure 13. TSLPR+ mono exhibit different phenotypic and functional properties. (A) Human peripheral blood or LPS-stimulated CD14+ monocytes were stained for CD14 and CD1c, and the percentages of CD1c- and CD1c+ among CD14+ cells were calculated. Right panels, representative contour plots. (B-E) Human CD14+ monocytes were stimulate with LPS and stained for CD14, CD1c and TSLPR. Percentage of TSLPR+ cells and TSLPR MFI were calculated in the indicated populations. (D) Representative histograms of TSLPR expression in unstained controls, CD14+ CD1c- and CD14+ CD1c+ cells. Data are shown as mean + SEM (A-C, E) of 6 (A-C, E) independent experiments. * p < 0.05, ** p < 0.01 determined by two-tailed paired t test (B, C, E), repeated measure two-way ANOVA with Sidak's post hoc test (A).

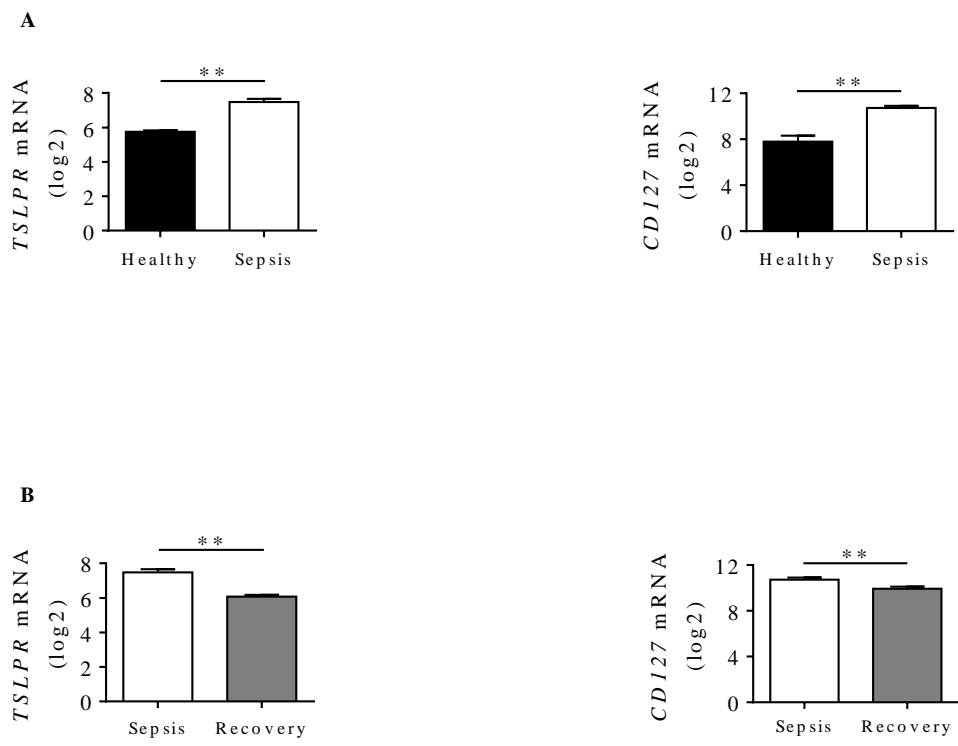
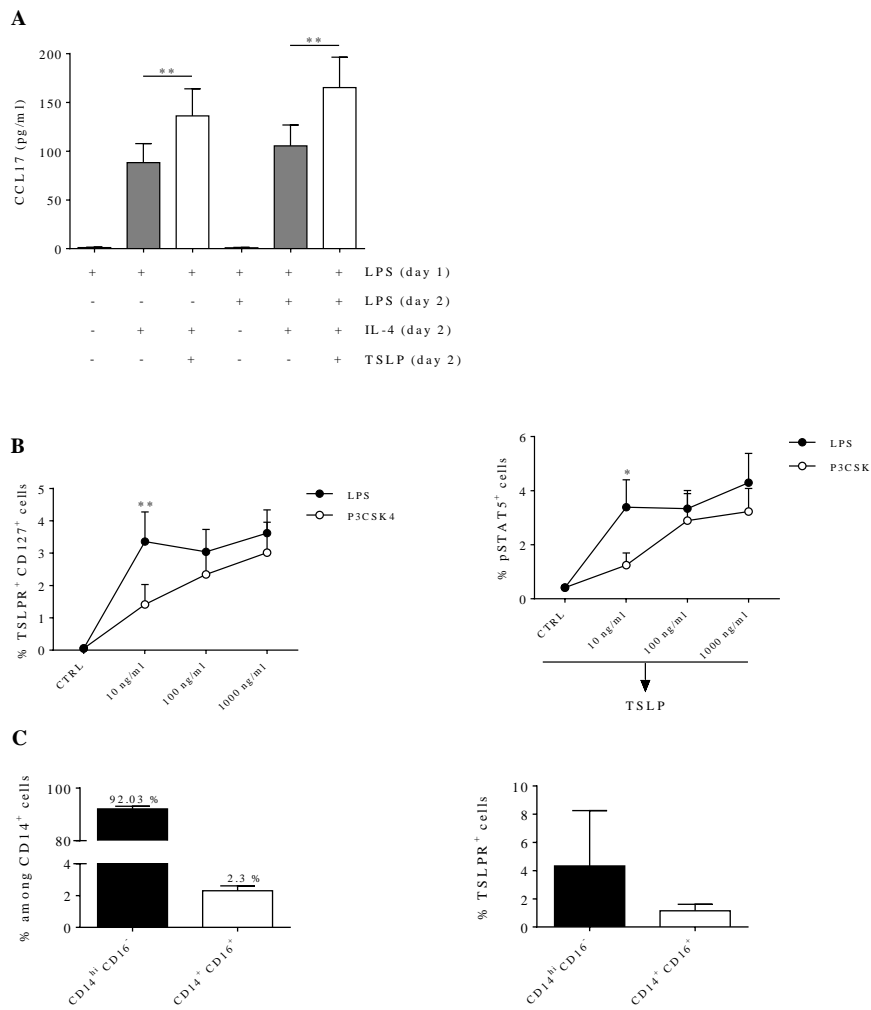
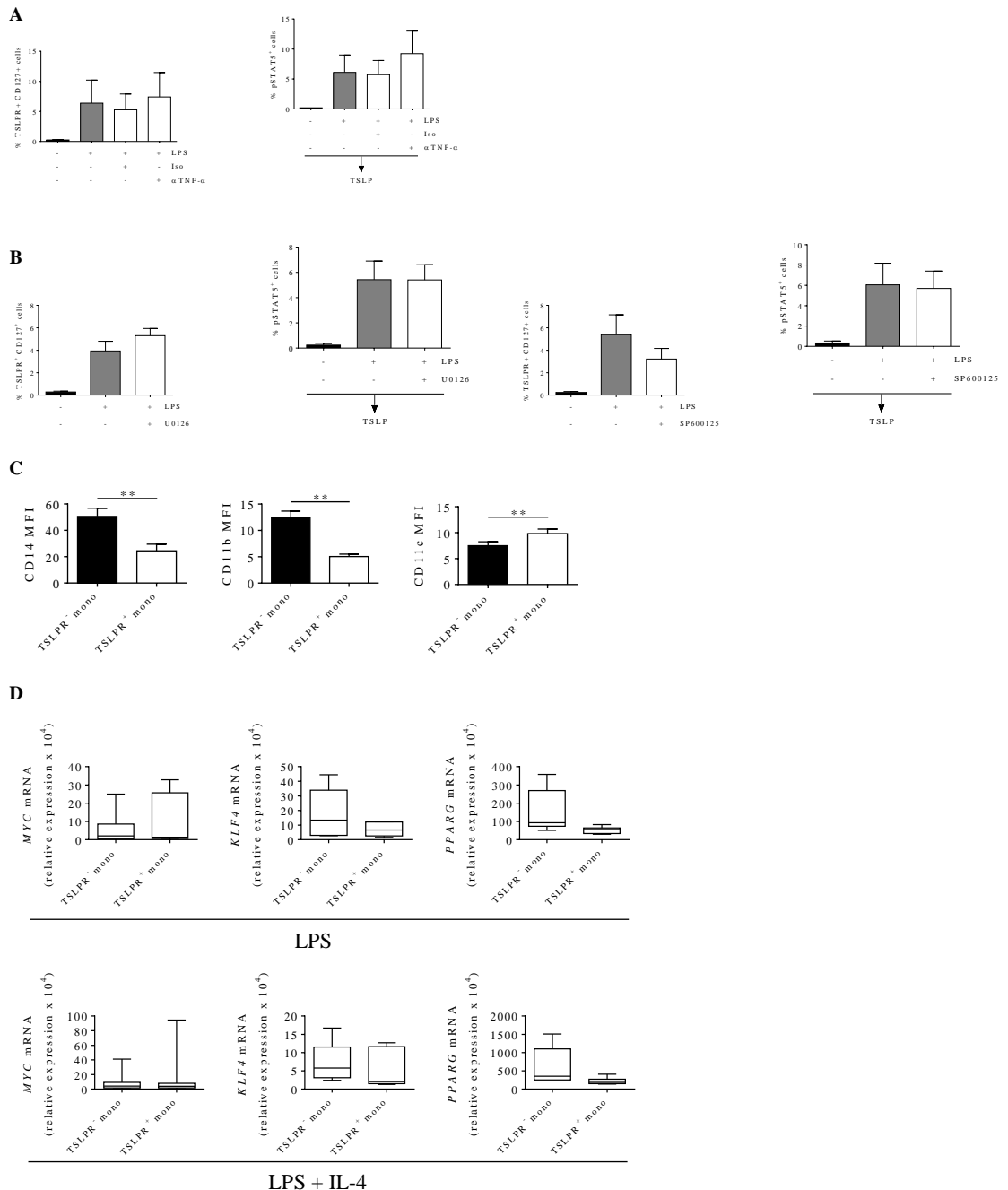


Figure 14. *In vivo* expression of *TSLPR* and *CD127* mRNAs. (A, B) Public available microarray (GSE46955) performed on peripheral blood human $CD14^+$ monocytes isolated from patients during Gram-negative sepsis (Sepsis, n=7) (A, B) and following their resolution or recovery (Recovery, n=7) (B) as well as from healthy donors (Healthy, n=5) (A) were analysed to assess *TSLPR* and *CD127* expression levels. ** $p < 0.01$ determined by two-tailed unpaired (A) or paired (B) t test.



Supplementary Figure 1. (A) Human CD14+ monocytes were pre-treated with LPS for 14 hours and then stimulated for 21-24 hours with IL-4 and TSLP in the presence or absence of LPS. CCL17 levels were assessed by ELISA in cell-free supernatants. (B) CD14+ human monocytes were stimulated with increasing concentrations (10, 100 and 1000 ng/ml) of LPS and P3CSK4 for 14 hours and the percentages of TSLPR+ CD127+ cells or pSTAT5+ cells in response to TSLP were assessed by flow cytometry. (C) Human CD14+ monocytes were sorted into CD14hi CD16- and CD14+ CD16+ and then stimulated overnight with LPS. The expression of TSLPR was assessed by flow cytometry. Numbers above bars represent means. Data are shown as mean + SEM of 21 (A), 6 (B) or 4 (C) independent experiments. * $p < 0.05$, ** $p < 0.01$ determined by repeated measure one-way ANOVA with Tukey's post hoc test (A) and repeated measure two-way ANOVA with Sidak's post hoc test (B).



Supplementary Figure 2 (A, B) Human CD14+ monocytes were stimulated with LPS in the presence or absence of α TNF- α (a blocking anti-TNF- α antibody) or an isotype control (Iso) (A), U0126 (MEK1/2 inhibitor) and SP600125 (JNK inhibitor) (B) for 14 hours and the percentages of TSLPR+ CD127+ cells or pSTAT5+ cells in response to TSLP were assessed by flow cytometry. (C) Human CD14+ monocytes were stimulated with LPS for 14 hours and the expression of CD14, CD11b and CD11c was assessed by flow cytometry as median fluorescence intensity (MFI). (D) Human CD14+ monocytes were pre-treated with LPS for 14 hours, FACS-sorted into TSLPR+ and TSLPR- mono and stimulated with LPS or LPS+IL-4 for 14 hours. Then, cells were harvested for RNA isolation and subsequent real time RT-PCR analysis. Data are shown as mean + SEM of 3 (A), 5 (B) or 6 (C) independent experiments, or as the median, the 25th and 75th percentiles (boxes) and the 5th and 95th percentiles (whiskers) of 6 independent experiments. (Figure legend continues)

Statistical significance was determined by repeated measure one-way ANOVA with Tukey's post hoc test (A, B), two-tailed paired t test (C) or Wilcoxon matched-pairs signed rank test (D). ** p < 0.01

Supplementary Table I

Upregulated gene transcripts in TSLPR ⁻ vs TSLPR ⁺						
Gene Symbol	Ensembl ID	logFC	PValue	FDR	TSLPR- 1	TSLPR- 2
SMAD3	ENSG00000166949	-3.11290	1.44E-05	0.007947	5.75806	2.28999
MYO10	ENSG00000145555	-1.85405	3.08E-05	0.013257	66.68877	31.16027
PPARG	ENSG00000132170	-2.31776	3.28E-05	0.013429	21.46185	5.64320
CARD16	ENSG00000204397	-1.38768	0.000219	0.04891	104.79664	45.06380
HS3ST2	ENSG00000122254	-3.63827	0.00027	0.058194	3.45483	0.24536
SNAPC1	ENSG00000023608	-1.74133	0.000472	0.084448	108.35617	25.84421
MMP10	ENSG00000166670	-2.97568	0.000503	0.087499	1127.63697	43.01916
CDCP1	ENSG00000163814	-1.92211	0.000549	0.092975	107.62332	14.63960
IGFN1	ENSG00000163395	-2.41703	0.000568	0.093775	128.66640	18.97423
CCND1	ENSG00000110092	-2.53959	0.000674	0.104056	15.28502	1.55392
GPRC5C	ENSG00000170412	-1.80167	0.00068	0.104056	10.36450	5.39784
CCDC17	ENSG00000159588	-1.70772	0.000925	0.127779	22.29938	7.44248
ZEB1	ENSG00000148516	-3.23303	0.001051	0.137245	15.18033	0.57250
NDRG4	ENSG00000103034	-3.43521	0.001204	0.151564	1.36100	0.32714
OLIG2	ENSG00000205927	-1.58629	0.001376	0.168187	47.42545	21.83672
AEN	ENSG00000181026	-1.92216	0.001508	0.175823	78.10019	14.63960
RGS17	ENSG0000091844	-3.21136	0.001543	0.177988	1.36100	0.16357
SPINK1	ENSG00000164266	-1.80693	0.001635	0.185477	203.62584	53.48770
NCOR2	ENSG00000196498	-1.24418	0.00165	0.185559	321.19490	157.27347
CD244	ENSG00000122223	-2.77480	0.002041	0.22166	16.22725	1.63571
CD109	ENSG00000156535	-1.45169	0.002097	0.225877	163.42413	112.20967
DUSP16	ENSG00000111266	-2.08920	0.002184	0.228057	150.65171	24.94457
SH2D5	ENSG00000189410	-4.31300	0.002425	0.238898	3.14076	0.08179
PLPP3	ENSG00000162407	-1.93046	0.002551	0.24564	185.30475	27.64349
WHRN	ENSG00000095397	-1.58704	0.002829	0.266053	9.73635	4.98891
SYPL2	ENSG00000143028	-2.02654	0.002897	0.268701	2.30322	1.47214
AICDA	ENSG00000111732	-3.23756	0.003166	0.28475	0.52346	0.24536
TFPI2	ENSG00000105825	-3.13477	0.00331	0.28475	1222.80195	18.64709
EML5	ENSG00000165521	-2.38189	0.003265	0.28475	1.46569	0.73607
TNFSF8	ENSG00000106952	-2.33990	0.003194	0.28475	6.17682	2.37178
KCNJ14	ENSG00000182324	-2.29357	0.003274	0.28475	2.40791	0.81785
HIVEP3	ENSG00000127124	-2.48800	0.003746	0.307454	51.08967	3.68035
ADAMTSL4-	ENSG00000203804	-2.33114	0.003772	0.307454	7.11905	1.96285
DNHD1	ENSG00000179532	-1.19570	0.003774	0.307454	52.66005	26.25314
HCAR2	ENSG00000182782	-1.63431	0.004407	0.343573	16.75071	7.19712
IARS	ENSG00000196305	-1.52221	0.004399	0.343573	179.65138	38.35739
ASIC3	ENSG00000213199	-1.64902	0.004772	0.356253	5.23460	3.92570
C10orf128	ENSG00000204161	-1.56316	0.004793	0.356253	106.15763	16.27531
NPIPBP3	ENSG00000169246	-1.19534	0.004767	0.356253	11.83019	12.75853
PCSK6	ENSG00000140479	-1.54590	0.005122	0.37195	13.60995	4.17106
HCAR3	ENSG00000255398	-1.38073	0.00543	0.38555	45.33161	18.64709
ZNF365	ENSG00000138311	-1.49142	0.006091	0.42071	3.97829	4.57999
SLC23A2	ENSG00000089057	-1.14633	0.006014	0.42071	92.65237	111.88253
TEX10	ENSG00000136891	-1.12061	0.00609	0.42071	50.67090	20.69173
ACTN2	ENSG00000077522	-2.66853	0.006336	0.429437	0.94223	0.16357
SLC22A13	ENSG00000172940	-2.79511	0.00671	0.437588	1.46569	0.57250
PI3	ENSG00000124102	-1.53938	0.006741	0.437588	13.08649	16.35710
EPB41	ENSG00000159023	-0.99976	0.006723	0.437588	23.55569	23.22707

CDKN2A	ENSG00000147889	-2.23960	0.007112	0.451928	1.67507	0.32714
P2RX7	ENSG00000089041	-1.49521	0.007604	0.473355	210.43081	62.56589
SCMH1	ENSG00000010803	-1.24468	0.007951	0.490561	17.69294	8.17855
MPP6	ENSG00000105926	-1.51529	0.00817	0.501634	6.07213	2.94428
TRMT6	ENSG00000089195	-1.46725	0.008368	0.511302	64.59493	12.43139
SPRY1	ENSG00000164056	-3.06428	0.008687	0.515923	9.00351	0.24536
TRIM25	ENSG00000121060	-0.92152	0.008849	0.52066	856.27544	701.22866
IRS2	ENSG00000185950	-1.23255	0.009227	0.528084	218.91086	75.16085
CAPN2	ENSG00000162909	-0.94622	0.009308	0.528084	186.14228	171.09521
CCND2	ENSG00000118971	-2.17563	0.009728	0.53683	5.33929	0.65428
TNFRSF10B	ENSG00000120889	-1.10069	0.009757	0.53683	237.23195	109.59254
SLC25A34	ENSG00000162461	-1.02595	0.009757	0.53683	30.57005	17.33852
SYNJ2	ENSG00000078269	-1.68242	0.010528	0.564577	59.25564	12.92211
PAX8	ENSG00000125618	-1.04596	0.010929	0.577977	17.48356	18.56530
ARFGEF3	ENSG00000112379	-2.25655	0.01124	0.58338	0.73284	0.32714
SLC4A5	ENSG00000188687	-1.37123	0.011659	0.60235	3.03607	3.10785
KANK1	ENSG00000107104	-0.85305	0.01176	0.605081	51.50844	51.44306
DUSP8	ENSG00000184545	-1.82339	0.011919	0.610806	7.22374	1.14500
MELTF	ENSG00000163975	-1.19988	0.012231	0.619322	10.46919	8.34212
MYEOV	ENSG00000172927	-2.66604	0.012808	0.627747	3.24545	0.08179
MIA	ENSG00000261857	-1.67167	0.012601	0.627747	2.19853	1.39035
AARS	ENSG00000090861	-1.22622	0.012722	0.627747	220.06247	76.79656
FAM83G	ENSG00000188522	-1.14003	0.012773	0.627747	33.92019	15.37567
TCP11L2	ENSG00000166046	-0.99188	0.013051	0.627747	14.86626	13.98532
AATK	ENSG00000181409	-0.95344	0.012943	0.627747	18.11171	18.64709
NPIPB4	ENSG00000185864	-0.85508	0.013083	0.627747	26.06829	26.00778
ZCCHC14	ENSG00000140948	-0.84254	0.013069	0.627747	100.08550	67.30945
JAG1	ENSG00000101384	-1.62305	0.013603	0.639408	67.10754	10.30497
CHD7	ENSG00000171316	-1.01528	0.014712	0.672552	15.91318	14.96674
KLF4	ENSG00000136826	-1.39181	0.014798	0.674072	13.60995	5.80677
C5orf56	ENSG00000197536	-1.12691	0.015576	0.692168	10.57389	9.32354
HMGA2	ENSG00000149948	-1.62042	0.015778	0.693261	16.96010	3.43499
PRNP	ENSG00000171867	-0.92703	0.015874	0.693261	151.59394	71.48051
ID2	ENSG00000115738	-0.90394	0.015843	0.693261	107.83271	45.88165
PPRC1	ENSG00000148840	-0.88673	0.015815	0.693261	78.10019	40.32024
EPS8	ENSG00000151491	-1.72980	0.015981	0.695558	7.74720	1.22678
MYBBP1A	ENSG00000132382	-1.04551	0.0162	0.697809	29.31375	16.92959
APOL6	ENSG00000221963	-0.94356	0.016332	0.698877	103.01688	76.14228
CDRT1	ENSG00000241322	-2.25214	0.017072	0.711592	0.31408	0.89964
NIPAL4	ENSG00000172548	-1.86420	0.017024	0.711592	15.80848	1.63571
CRYM	ENSG00000103316	-1.81166	0.017426	0.711592	1.04692	0.73607
FNDC3A	ENSG00000102531	-1.05784	0.017461	0.711592	281.62134	93.88973
ITPR1	ENSG00000150995	-1.04614	0.017079	0.711592	226.02991	113.02753
COA7	ENSG00000162377	-1.00895	0.017248	0.711592	26.17299	13.65817
TTF2	ENSG00000116830	-0.91828	0.016941	0.711592	12.87711	14.96674
HMGA1	ENSG00000137309	-0.87215	0.017469	0.711592	130.76024	104.68541
ZC3H12C	ENSG00000149289	-1.06638	0.0176	0.714631	241.00086	109.91968
USP36	ENSG00000055483	-0.97006	0.018154	0.730049	110.45000	49.72557
FBXO31	ENSG00000103264	-0.98591	0.018593	0.738441	17.48356	10.87747
MFAP5	ENSG00000197614	-1.72401	0.019106	0.742926	2.93137	3.84392

CTRL	ENSG00000141086	-1.14227	0.019174	0.742926	11.09735	6.13391
CABLES1	ENSG00000134508	-1.82303	0.019551	0.746053	3.03607	0.65428
RCL1	ENSG00000120158	-1.32000	0.019569	0.746053	4.18768	2.12642
TSPOAP1	ENSG00000005379	-1.27663	0.019665	0.746053	5.44398	3.43499
NFIX	ENSG00000008441	-1.62458	0.020191	0.754711	0.83754	1.39035
ATP2B1	ENSG00000070961	-1.26024	0.020184	0.754711	1141.24692	294.42771
CHD9	ENSG00000177200	-0.81777	0.020107	0.754711	30.98882	25.84421
EDN1	ENSG00000078401	-2.49085	0.020524	0.76092	62.29171	1.88107
EIF5AL1	ENSG00000253626	-1.65323	0.020464	0.76092	1.25630	1.22678
ARHGAP15	ENSG00000075884	-1.75588	0.021752	0.778354	27.21991	5.80677
RP11-513I15.6	ENSG00000225339	-1.35054	0.021908	0.778354	3.24545	1.71749
CAMKK2	ENSG00000110931	-0.66487	0.021984	0.778354	61.03541	66.73695
GBP5	ENSG00000154451	-1.34588	0.022687	0.796478	14.23810	4.00749
GNRH2	ENSG00000125787	-2.33070	0.023524	0.808567	0.52346	0.24536
GPRC5A	ENSG00000013588	-1.96645	0.023625	0.809295	0.62815	0.49071
UBR4	ENSG00000127481	-0.86392	0.023833	0.81203	726.56212	534.14094
ZFYVE9	ENSG00000157077	-1.36372	0.024203	0.818059	14.65687	3.59856
ZNF117	ENSG00000152926	-0.77372	0.024087	0.818059	51.92721	35.41311
P2RX4	ENSG00000135124	-0.92046	0.024334	0.818148	325.48727	134.37354
IRF1	ENSG00000125347	-0.82999	0.02478	0.828762	167.92588	90.20938
TNXB	ENSG00000168477	-1.97756	0.025364	0.829555	0.52346	0.32714
XYLB	ENSG00000093217	-1.46349	0.025129	0.829555	1.67507	1.14500
STEAP4	ENSG00000127954	-1.41706	0.025892	0.829555	10.99265	5.64320
KCNA3	ENSG00000177272	-1.35309	0.0254	0.829555	1.88446	1.39035
PMEPA1	ENSG00000124225	-1.29193	0.025592	0.829555	6.90967	3.27142
NCR3LG1	ENSG00000188211	-0.99101	0.025812	0.829555	70.14360	32.71419
DGKE	ENSG00000153933	-0.79151	0.025291	0.829555	56.95242	39.01167
PLA2G4A	ENSG00000116711	-0.71224	0.025114	0.829555	76.73920	71.72586
TNRC6C	ENSG00000078687	-0.96586	0.02608	0.83233	17.69294	11.04104
C19orf71	ENSG00000183397	-1.73225	0.026542	0.83251	2.72199	0.73607
DRICH1	ENSG00000189269	-1.56242	0.02725	0.83251	0.94223	1.30857
DGKD	ENSG00000077044	-1.32844	0.026699	0.83251	175.46370	36.39454
DDX43	ENSG00000080007	-1.18785	0.026812	0.83251	2.51261	2.78071
MAML2	ENSG00000184384	-0.97855	0.027043	0.83251	142.59043	54.22377
XPOT	ENSG00000184575	-0.72991	0.026295	0.83251	102.70280	64.52874
SH3D21	ENSG00000214193	-0.69455	0.026983	0.83251	65.74654	81.29476
ZBTB11	ENSG00000066422	-0.74590	0.027447	0.836518	48.99583	31.48741
F3	ENSG00000117525	-2.16053	0.028526	0.837945	1047.54763	44.65487
GPD1	ENSG00000167588	-1.74336	0.027869	0.837945	1.15161	0.40893
STOX2	ENSG00000173320	-1.57527	0.027977	0.837945	0.62815	7.27891
CD22	ENSG00000012124	-1.27749	0.027787	0.837945	6.80498	5.23427
JARID2	ENSG00000008083	-0.95966	0.029474	0.845571	582.50600	244.86571
KLF10	ENSG00000155090	-0.78111	0.030058	0.851902	94.32744	72.21657
TIPARP	ENSG00000163659	-1.03045	0.030168	0.852008	348.20542	204.30012
TMEM158	ENSG00000249992	-1.17883	0.030451	0.853832	15.70379	5.72498
CCDC88B	ENSG00000168071	-0.99362	0.030453	0.853832	37.27033	28.29777
HIVEP2	ENSG00000010818	-0.81215	0.030736	0.856489	257.22812	176.57484
RIMKLB	ENSG00000166532	-0.76106	0.031108	0.859465	41.56270	29.03384
RBM19	ENSG00000122965	-0.76382	0.031661	0.86721	91.71015	49.39843
CDKN2B	ENSG00000147883	-1.33418	0.03205	0.868998	140.60129	26.08957

LRP3	ENSG00000130881	-1.08697	0.032012	0.868998	4.18768	4.57999
RBM28	ENSG00000106344	-0.71399	0.032308	0.87178	45.75038	33.61383
AK4	ENSG00000162433	-0.72938	0.032897	0.880173	197.65840	178.37412
FAM208B	ENSG00000108021	-0.71693	0.033104	0.880306	81.03157	57.74055
ABCE1	ENSG00000164163	-0.78373	0.033454	0.883933	48.36768	24.04493
CYP1A1	ENSG00000140465	-1.97259	0.033695	0.886547	74.95943	10.87747
FAM129A	ENSG00000135842	-0.75713	0.033672	0.886547	378.14731	286.57630
TAF4B	ENSG00000141384	-1.32418	0.034131	0.890697	3.66422	2.20821
SUMO4	ENSG00000177688	-2.03467	0.034295	0.892625	0.10469	0.57250
MGEA5	ENSG00000198408	-0.75160	0.034345	0.892625	300.15181	210.84295
AFAP1	ENSG00000196526	-1.48055	0.034517	0.893502	7.53782	5.64320
BTN3A1	ENSG00000026950	-0.91212	0.03459	0.893502	29.41844	17.25674
DBN1	ENSG00000113758	-1.24702	0.035003	0.895065	7.32844	3.59856
NKX3-1	ENSG00000167034	-1.14152	0.034863	0.895065	34.44365	15.53924
TRIM22	ENSG00000132274	-0.89535	0.034873	0.895065	26.69645	31.32384
SLC9A8	ENSG00000197818	-0.67522	0.035204	0.896201	117.98782	96.99757
COL1A2	ENSG00000164692	-2.13734	0.036415	0.897373	4.60645	0.40893
DQX1	ENSG00000144045	-1.85822	0.037153	0.897373	0.83754	0.65428
ADORA2B	ENSG00000170425	-1.66084	0.035777	0.897373	2.30322	0.49071
PTGER3	ENSG00000050628	-1.64948	0.03821	0.897373	0.94223	0.89964
CUBN	ENSG00000107611	-1.41988	0.036237	0.897373	3.35014	1.39035
SPAG5-AS1	ENSG00000227543	-1.40625	0.035946	0.897373	12.14427	2.37178
ANKRD33B	ENSG00000164236	-1.31128	0.036936	0.897373	63.54801	13.16746
CCDC88C	ENSG00000015133	-1.30739	0.03733	0.897373	32.34981	6.95177
CASP1	ENSG00000137752	-1.09221	0.037563	0.897373	729.49349	219.67579
PHACTR1	ENSG00000112137	-1.00431	0.036127	0.897373	182.79214	79.49548
AGAP6	ENSG00000204149	-0.78666	0.038377	0.897373	35.28119	20.11923
KLHL21	ENSG00000162413	-0.77303	0.038028	0.897373	208.75574	134.45532
HIVEP1	ENSG00000095951	-0.73266	0.036921	0.897373	147.19688	124.31392
POFUT2	ENSG00000186866	-0.72310	0.037468	0.897373	86.99901	55.77769

Gene Symbol	TSLPR⁻ 3	TSLPR⁺ 1	TSLPR⁺ 2	TSLPR⁺ 3
SMAD3	6.82057	0.29515	1.18821	0.28575
MYO10	50.53156	8.85463	24.03833	10.00125
PPARG	20.75827	2.55800	3.01622	4.28625
CARD16	79.77106	26.66228	29.24815	34.29001
HS3ST2	5.21922	0.29515	0.27420	0.14288
SNAPC1	105.27408	29.90898	26.32334	16.50207
MMP10	308.58649	95.43325	79.24421	25.21744
CDCP1	66.54508	18.00442	17.18329	16.85925
IGFN1	43.11789	9.64171	25.22653	3.92906
CCND1	8.30331	1.96770	1.37101	1.14300
GPRC5C	12.09911	3.44347	2.46781	2.07169
CCDC17	17.25902	6.09986	4.66142	3.85763
ZEB1	3.38063	1.18062	0.45700	0.50006
NDRG4	12.33634	0.39354	0.18280	0.64294
OLIG2	51.24327	12.88841	5.57543	22.00276
AEN	30.30707	17.31572	10.51105	5.64356
RGS17	1.83859	0.09838	0.18280	0.07144
SPINK1	88.07437	58.14542	26.14054	15.50194
NCOR2	311.96712	136.16456	101.36313	97.36933
CD244	3.38063	2.06608	0.73120	0.42863
CD109	486.21796	98.58157	89.66387	84.22483
DUSP16	30.12914	28.23644	14.34987	7.71525
SH2D5	0.77102	0.19677	0.00000	0.00000
PLPP3	53.43771	40.23938	15.17248	16.78782
WHRN	11.09085	3.24670	3.56462	1.85738
SYPL2	6.99850	0.59031	1.18821	0.85725
AICDA	1.06757	0.00000	0.18280	0.00000
TFPI2	152.84017	116.78275	19.10270	29.71801
EML5	1.48273	0.09838	0.54840	0.07144
TNFSF8	1.36411	0.98385	0.82260	0.21431
KCNJ14	1.42342	0.29515	0.36560	0.28575
HIVEP3	13.70046	8.55948	1.37101	2.57175
ADAMTSL4-AS1	2.96547	1.67254	0.45700	0.28575
DNHD1	46.73576	22.13658	22.02751	11.21569
HCAR2	33.39116	5.90309	2.92482	9.50119
IARS	95.72527	56.76803	29.06535	25.50319
ASIC3	5.39715	2.26285	1.64521	0.71438
C10orf128	82.79584	25.67843	15.17248	30.71813
NPIPBP3	21.76653	7.57563	6.39803	5.92931
PCSK6	19.92794	3.24670	4.84423	5.07206
HCAR3	75.02631	19.57857	9.23145	24.21732
ZNF365	8.83709	1.37739	3.10762	1.71450
SLC23A2	285.51516	74.37891	56.21129	84.65346
TEX10	46.08336	21.05435	17.09189	16.50207
ACTN2	2.60961	0.00000	0.27420	0.28575
SLC22A13	0.59309	0.29515	0.00000	0.07144
PI3	24.43545	1.08223	8.68305	9.14400
EPB41	34.34011	13.87226	16.08648	10.35844

CDKN2A	1.66066	0.19677	0.36560	0.21431
P2RX7	217.84320	100.35249	44.69483	26.28901
SCMH1	13.16667	6.09986	5.94103	4.71488
MPP6	4.98198	1.47577	2.46781	1.07156
TRMT6	37.54281	20.36565	8.77445	13.14450
SPRY1	1.42342	0.98385	0.27420	0.07144
TRIM25	1099.47653	448.73306	557.08590	399.04997
IRS2	104.85891	80.97069	51.91547	40.29076
CAPN2	358.16910	101.82827	149.98818	118.65771
CCND2	5.21922	1.08223	0.18280	1.21444
TNFRSF10B	109.60366	79.79007	88.74986	50.86351
SLC25A34	33.80632	13.97064	15.72088	10.78706
SYNJ2	32.26428	20.66081	8.68305	3.28613
PAX8	14.64941	8.06755	11.05946	5.50069
ARFGEF3	1.77928	0.09838	0.18280	0.28575
SLC4A5	3.55856	0.78708	1.91941	1.07156
KANK1	83.38893	32.95891	44.87763	24.78882
DUSP8	8.65916	1.86931	0.82260	2.14313
MELTF	10.49775	2.95154	6.85504	3.21469
MYEOV	1.54204	0.39354	0.09140	0.28575
MIA	2.43168	0.88546	0.73120	0.28575
AARS	113.57738	89.23501	54.01768	34.50432
FAM83G	23.72374	15.44641	9.14005	8.71538
TCP11L2	18.62313	7.08371	10.60246	6.28650
AATK	26.33335	11.90456	8.40884	11.78719
NPIPB4	32.14566	15.74157	17.54889	13.07307
ZCCHC14	83.74479	56.57126	42.86682	40.71938
JAG1	14.76803	16.03672	7.58624	7.64381
CHD7	23.90166	8.65786	12.43046	6.00075
KLF4	14.94595	6.98532	2.19361	3.71475
C5orf56	18.44520	6.00147	7.76904	3.71475
HMGA2	8.30331	4.52570	3.74742	1.35731
PRNP	122.88895	75.75629	57.12530	50.57776
ID2	83.50755	41.91192	37.93120	49.86339
PPRC1	65.00304	40.23938	28.88255	30.71813
EPS8	7.71021	2.36124	1.73661	1.00013
MYBBP1A	23.72374	15.34803	7.86044	10.57275
APOL6	158.77110	63.26142	79.06141	32.57551
CDRT1	1.48273	0.39354	0.09140	0.07144
NIPAL4	8.83709	3.73862	2.92482	0.78581
CRYM	1.24550	0.09838	0.54840	0.21431
FNDC3A	266.95134	128.49055	86.46485	96.51208
ITPR1	267.12926	109.50228	133.71890	52.36370
COA7	20.69896	12.19971	9.32285	8.78681
TTF2	18.91968	8.26432	8.59164	7.64381
HMGA1	218.43630	78.80622	65.53414	101.94134
ZC3H12C	134.27634	113.14252	71.47517	48.86326
USP36	79.71175	57.75188	31.25896	33.78995
FBXO31	13.87839	6.49340	7.22064	7.92956
MFAP5	21.35136	0.88546	3.19902	4.35769

CTRL	10.97223	4.82086	4.84423	3.21469
CABLES1	1.36411	0.39354	0.63980	0.42863
RCL1	4.27027	1.47577	1.27961	1.50019
TSPOAP1	6.82057	2.75477	2.28501	1.42875
NFIX	1.00826	0.19677	0.54840	0.28575
ATP2B1	485.68418	414.59354	246.68989	159.80572
CHD9	45.25303	18.20119	23.67272	16.07344
EDN1	3.49925	8.95302	2.65061	1.07156
EIF5AL1	2.66892	0.39354	0.18280	1.00013
ARHGAP15	4.80406	6.88694	3.47322	1.21444
RP11-513I15.6	5.45646	1.08223	1.37101	1.64306
CAMKK2	67.73127	36.00884	44.60343	42.71963
GBP5	11.74325	5.60793	4.11302	2.21456
GNRH2	0.59309	0.00000	0.09140	0.14288
GPRC5A	3.43994	0.49192	0.36560	0.28575
UBR4	851.50418	440.46874	464.58862	252.10300
ZFYVE9	13.52253	5.90309	4.20442	2.35744
ZNF117	50.47225	26.85905	32.90417	21.64557
P2RX4	220.57143	143.54342	110.50318	112.01403
IRF1	136.23355	85.20123	69.55576	69.29439
TNXB	1.54204	0.19677	0.18280	0.21431
XYLB	1.77928	0.59031	0.73120	0.35719
STEAP4	3.55856	3.83701	1.18821	2.57175
KCNA3	2.66892	0.78708	0.82260	0.71438
PMEPA1	9.72673	3.64024	2.74201	1.71450
NCR3LG1	56.16594	40.23938	24.12973	15.35907
DGKE	45.78681	32.27021	29.15675	20.78832
PLA2G4A	66.01129	44.86347	53.56068	32.86126
TNRC6C	11.86187	7.28047	7.95184	5.85788
C19orf71	1.06757	0.39354	0.63980	0.35719
DRICH1	1.42342	0.39354	0.63980	0.21431
DGKD	44.77855	57.25995	28.33415	20.00250
DDX43	4.56682	1.37739	1.64521	1.28588
MAML2	81.13518	65.32751	48.07665	29.93232
XPOT	101.24104	54.80033	58.67911	49.93482
SH3D21	79.83037	43.19093	62.15232	34.29001
ZBTB11	46.32059	23.71074	29.06535	23.86013
F3	121.22829	215.26594	43.41523	21.50269
GPD1	1.30481	0.29515	0.18280	0.35719
STOX2	5.51577	1.08223	2.10221	1.14300
CD22	3.38063	2.85316	1.09681	2.35744
JARID2	537.10538	327.32622	182.16115	190.80961
KLF10	130.77709	71.23059	60.78132	38.79057
TIPARP	519.37188	271.34527	92.22308	145.08960
TMEM158	14.29355	3.04993	4.02162	9.21544
CCDC88B	20.63965	19.38181	17.27469	6.71513
HIVEP2	231.18780	152.59482	143.31595	83.08183
RIMKLB	42.10963	23.21881	27.14594	16.57350
RBM19	68.85814	48.60209	38.29680	38.00476
CDKN2B	49.40468	51.55363	23.30712	12.71588

LRP3	3.20270	1.67254	2.01081	1.92881
RBM28	51.36189	27.94128	28.15135	23.71726
AK4	186.40925	111.96190	144.96116	83.86764
FAM208B	88.01506	53.22618	49.17346	35.29013
ABCE1	46.32059	23.12043	21.93611	24.86026
CYP1A1	40.74552	27.64613	1.18821	2.42888
FAM129A	575.65645	218.51263	278.49725	238.45843
TAF4B	2.37237	1.67254	0.82260	0.78581
SUMO4	1.12688	0.09838	0.18280	0.14288
MGEA5	423.82454	171.18955	201.35525	184.52310
AFAP1	2.19445	2.85316	2.10221	0.57150
BTN3A1	25.62163	15.44641	15.81228	7.42950
DBN1	5.51577	3.54185	2.10221	1.28588
NKX3-1	12.92944	14.06903	10.51105	4.42913
TRIM22	26.45197	12.69164	25.50073	7.57238
SLC9A8	137.83490	77.33045	76.04520	67.07983
COL1A2	1.77928	0.98385	0.00000	0.57150
DQX1	0.41517	0.00000	0.27420	0.21431
ADORA2B	1.60135	0.68869	0.27420	0.42863
PTGER3	0.65240	0.09838	0.54840	0.14288
CUBN	7.88814	2.16447	1.18821	1.28588
SPAG5-AS1	4.21096	3.24670	2.37641	1.71450
ANKRD33B	17.49626	22.53012	8.31744	8.07244
CCDC88C	12.98875	12.29810	5.20983	4.00050
CASP1	298.14805	308.23957	164.61226	123.37259
PHACTR1	103.96927	97.59772	53.65208	31.57538
AGAP6	34.34011	19.77534	14.71548	17.71650
KLHL21	175.14048	126.91639	101.82013	74.72364
HIVEP1	126.86268	88.44793	96.33610	55.36408
POFUT2	67.96850	52.04556	42.13562	33.93282

Supplementary Table II

Upregulated gene transcripts in TSLPR ⁺ vs TSLPR ⁻						
Gene_Symbol	Ensembl_ID	logFC	PValue	FDR	TSLPR ⁻ 1	TSLPR ⁻ 2
CCR7	ENSG0000001	5.92136	8.48E-33	1.08E-28	2.09384	0.98143
CRLF2	ENSG0000002	4.31192	1.22E-15	7.73E-12	0.62815	2.69892
LAMP3	ENSG0000000	2.92873	9.05E-14	3.84E-10	5.12991	8.34212
MMP12	ENSG0000002	5.05779	2.99E-09	9.48E-06	0.10469	0.00000
LAD1	ENSG0000001	2.92657	5.50E-09	1.40E-05	2.30322	3.68035
MMP7	ENSG0000001	3.57325	1.07E-07	0.00022674	0.00000	0.65428
SORBS3	ENSG0000001	1.93634	2.30E-07	0.000417	5.65337	9.15997
HLA-DPA1	ENSG0000002	3.20816	7.36E-07	0.00116933	1.46569	4.49820
TNNT2	ENSG0000001	4.72354	1.55E-06	0.0021818	0.00000	0.32714
CD1C	ENSG0000001	2.90283	2.06E-06	0.00262088	0.52346	0.98143
C1QC	ENSG0000001	4.42795	3.81E-06	0.00372442	0.00000	0.08179
CD86	ENSG0000001	2.31629	3.71E-06	0.00372442	6.70028	5.39784
FCRLB	ENSG0000001	1.81799	3.29E-06	0.00372442	6.07213	9.89604
GCSAM	ENSG0000001	7.38957	4.38E-06	0.00397431	0.00000	0.00000
HLA-DMA	ENSG0000002	2.23696	4.87E-06	0.00412571	2.51261	6.54284
CD1E	ENSG0000001	4.63580	5.24E-06	0.00416554	0.00000	0.08179
NCCRP1	ENSG0000001	3.37687	5.73E-06	0.00428214	0.31408	0.57250
PALLD	ENSG0000001	2.79352	6.08E-06	0.00429124	1.88446	0.98143
MRC1	ENSG0000002	2.14711	6.86E-06	0.00453111	55.69612	61.58446
FCGR2B	ENSG0000000	1.90329	7.13E-06	0.00453111	28.99967	53.48770
FBN1	ENSG0000001	4.86998	9.44E-06	0.00571561	0.00000	0.00000
CD74	ENSG0000000	2.21217	1.02E-05	0.00589131	25.23076	57.90412
HLA-DPB1	ENSG0000002	3.44168	1.95E-05	0.00991161	0.20938	2.12642
TFRC	ENSG0000000	1.44415	1.94E-05	0.00991161	89.93038	149.99456
SLC22A23	ENSG0000001	3.19985	2.25E-05	0.01100605	0.52346	0.32714
EMP2	ENSG0000002	3.00482	2.41E-05	0.01135161	0.41877	0.24536
CXCL13	ENSG0000001	4.83078	2.75E-05	0.01248542	0.00000	0.24536
CALCRL	ENSG0000000	3.45618	3.13E-05	0.01325742	0.10469	0.00000
TSPAN15	ENSG0000000	6.32592	3.48E-05	0.01383548	0.00000	0.00000
CST7	ENSG0000000	4.47423	3.77E-05	0.01452565	0.00000	0.16357
GAS6	ENSG0000001	2.18668	4.21E-05	0.01574797	0.73284	1.22678
C1QB	ENSG0000001	4.71325	8.44E-05	0.02820578	0.00000	0.00000
CLEC4F	ENSG0000001	3.54810	8.66E-05	0.02820578	0.00000	0.16357
HLA-DMB	ENSG0000002	2.52745	8.16E-05	0.02820578	0.73284	4.00749
MGAT4A	ENSG0000000	1.51420	8.49E-05	0.02820578	10.88796	36.39454
CYP2S1	ENSG0000001	1.48732	7.80E-05	0.02820578	6.90967	18.48352
NAV2	ENSG0000001	1.70002	9.38E-05	0.02978677	3.03607	8.09676
HLA-DRA	ENSG0000002	2.10949	9.85E-05	0.03053022	17.27417	45.96344
ZNF366	ENSG0000001	3.38549	0.0001202	0.03568927	0.00000	0.08179
CYP27B1	ENSG0000001	2.29316	0.0001207	0.03568927	2.61730	17.82923
ROBO1	ENSG0000001	3.06709	0.0001240	0.03582306	0.00000	0.40893
MT1E	ENSG0000001	1.51442	0.0001303	0.0368062	13.50526	19.21959

TVP23A	ENSG000001	5.1878	0.0001434	0.03964002	0.00000	0.00000
FBP1	ENSG000001	2.2714	0.0001512	0.04088921	10.25981	10.30497
GFPT2	ENSG000001	2.3011	0.0001549	0.04102642	0.52346	2.94428
ENTHD1	ENSG000001	2.6134	0.0001767	0.04561564	0.10469	0.32714
CPED1	ENSG000001	2.2408	0.0001852	0.04561564	1.04692	1.22678
HLA-DRB1	ENSG000001	2.0232	0.0001804	0.04561564	15.18033	33.69562
ENO2	ENSG000001	1.5043	0.0001866	0.04561564	17.48356	39.09346
ENTPD1	ENSG000001	2.9678	0.0001958	0.04660244	0.00000	0.32714
MT1X	ENSG000001	1.6343	0.0001980	0.04660244	10.78327	26.98921
ALOX15B	ENSG000001	1.9749	0.0002036	0.04704797	2.09384	4.66177
RTN1	ENSG000001	1.9404	0.0002141	0.04858886	2.72199	16.35710
EHF	ENSG000001	2.0019	0.0002662	0.05819395	1.57038	2.53535
ITIH1	ENSG000000	1.7273	0.000286	0.05935358	1.88446	7.52426
TCF4	ENSG000001	1.5871	0.0002892	0.05935358	2.51261	4.17106
PTGIR	ENSG000001	1.1481	0.0002895	0.05935358	27.84806	57.90412
KCNE5	ENSG000001	2.2198	0.0003057	0.0597724	1.25630	0.57250
MT1M	ENSG000002	2.0295	0.0003047	0.0597724	2.51261	7.52426
CCL22	ENSG000001	2.6018	0.0003105	0.05979311	1.15161	0.32714
HLA-DRB5	ENSG000001	2.1443	0.0003544	0.06722693	4.29237	7.44248
EBI3	ENSG000001	1.8689	0.0003855	0.07206409	9.94574	29.85170
FPR2	ENSG000001	1.3926	0.0004334	0.07982752	20.20555	28.87027
HLA-DOA	ENSG000002	3.4820	0.0004565	0.08288058	0.00000	0.08179
GCKR	ENSG000000	2.2676	0.0004813	0.08496715	0.31408	2.86249
SPN	ENSG000001	1.5590	0.0005180	0.08896637	11.41142	15.62103
HIST1H1C	ENSG000001	1.4936	0.0005672	0.09377479	4.08299	13.65817
TNFRSF6B	ENSG000002	1.7890	0.0006256	0.10193309	4.81583	4.57999
MT1F	ENSG000001	1.5490	0.0006626	0.10405613	9.94574	31.07848
MOB3B	ENSG000001	1.1111	0.0006698	0.10405613	33.29204	31.24205
CTSH	ENSG000001	1.3854	0.0007232	0.10943096	388.40713	390.60743
VEGFA	ENSG000001	1.1675	0.0007560	0.11304357	28.26683	53.07877
ACE	ENSG000001	2.3426	0.0007670	0.11335514	0.10469	1.63571
HSD11B1	ENSG000001	2.9654	0.0007891	0.1152742	0.00000	0.65428
LAIR1	ENSG000001	1.3791	0.0008771	0.12525886	22.09000	83.74833
RYR1	ENSG000001	2.0419	0.0009060	0.12777915	0.31408	1.63571
PLXDC2	ENSG000001	1.2964	0.0009424	0.12878794	10.46919	35.57668
CORO1A	ENSG000001	1.2852	0.0010044	0.13580588	18.53047	59.37625
CCL24	ENSG000001	2.8445	0.0010583	0.13724468	5.75806	40.40202
HAS1	ENSG000001	1.9762	0.0010431	0.13724468	0.83754	1.63571
TSPAN33	ENSG000001	1.2626	0.0010536	0.13724468	32.45450	73.77050
MEP1A	ENSG000001	1.9371	0.0011441	0.14687817	0.62815	0.89964
ITGB2	ENSG000001	1.1887	0.0012436	0.15495688	297.22044	555.65052
CD1B	ENSG000001	2.6906	0.0014203	0.17191181	0.10469	0.00000
PARP15	ENSG000001	1.9592	0.0014555	0.17430946	0.94223	1.79928
SLC1A2	ENSG000001	1.9358	0.0014766	0.17430946	0.62815	3.18963

ADAMTS14	ENSG000001	1.15404	0.00148127	0.17430946	30.15128	92.49937
FLT3	ENSG000001	2.93720	0.0017672	0.19529911	0.00000	0.00000
PPBP	ENSG000001	1.81279	0.00213493	0.22686723	2.61730	14.47603
CLIC2	ENSG000001	1.32997	0.00214211	0.22686723	5.23460	4.00749
PECAM1	ENSG000002	1.74072	0.00218924	0.22805741	1.46569	10.87747
CD207	ENSG000001	3.14747	0.00222798	0.23020697	0.00000	0.00000
CLEC6A	ENSG000002	2.77355	0.00224626	0.23022374	0.00000	1.06321
RARRES1	ENSG000001	4.21766	0.00237821	0.23798973	0.00000	0.08179
TIAM1	ENSG000001	1.07797	0.00234485	0.23798973	12.77242	23.39065
CLEC10A	ENSG000001	3.06278	0.00240479	0.23876914	0.00000	1.71749
A2M	ENSG000001	2.34654	0.00249002	0.24342825	7.64251	0.98143
TMEM173	ENSG000001	1.40243	0.00252957	0.2454066	3.14076	12.67675
FPR1	ENSG000001	1.60648	0.00260164	0.24860323	17.79763	28.95206
CYGB	ENSG000001	2.65923	0.00272464	0.25841357	0.10469	0.16357
ITGA4	ENSG000001	1.43868	0.00284705	0.26605279	1.77976	3.51678
CCR6	ENSG000001	2.63174	0.00295308	0.271962	0.00000	0.16357
ADCY6	ENSG000001	1.94074	0.00301071	0.27527437	0.20938	0.65428
PTPRF	ENSG000001	2.25034	0.00324146	0.28474982	0.20938	1.88107
GSN	ENSG000001	1.58351	0.00322994	0.28474982	33.18735	85.30225
ZNF395	ENSG000001	1.23883	0.0033302	0.28474982	9.84104	21.10065
ACTG1	ENSG000001	1.13673	0.00321323	0.28474982	228.75191	266.45708
STEAP3	ENSG000001	1.07952	0.00337314	0.28579533	22.09000	53.65127
TIFAB	ENSG000002	2.48691	0.00351235	0.29561865	0.00000	1.39035
FAM124A	ENSG000001	1.10765	0.00360654	0.30154922	6.70028	10.87747
LMO2	ENSG000001	1.15810	0.00367568	0.30532145	8.37536	12.10425
NDRG2	ENSG000001	2.75010	0.00383021	0.30808952	0.10469	0.98143
TNFAIP8L2	ENSG000001	1.05979	0.00381707	0.30808952	9.94574	24.04493
CP	ENSG000000	3.20056	0.00386065	0.30858521	0.00000	0.16357
HNMT	ENSG000001	1.22254	0.00400587	0.31819163	18.73986	65.67374
UGCG	ENSG000001	0.83322	0.00411217	0.3246062	37.47972	51.52485
TREM2	ENSG000000	3.57751	0.00464316	0.35625298	0.10469	0.16357
INSM1	ENSG000001	2.61161	0.0046601	0.35625298	0.00000	0.24536
C1orf54	ENSG000001	2.15448	0.00471532	0.35625298	0.31408	0.65428
FABP5	ENSG000001	1.63150	0.0047066	0.35625298	2.19853	2.53535
TNFSF13	ENSG000001	1.52666	0.00477398	0.35625298	8.79412	9.32354
KCP	ENSG000001	1.83386	0.00497715	0.36563332	0.83754	1.55392
ALDH2	ENSG000001	1.72255	0.00494882	0.36563332	1.88446	9.56890
SPRED1	ENSG000001	0.93333	0.00502824	0.36726414	24.70730	37.37596
MROH7	ENSG000001	2.49341	0.00541536	0.38555004	0.00000	0.08179
PPP1R14C	ENSG000001	2.35638	0.00542516	0.38555004	0.00000	0.16357
RAB3D	ENSG000001	1.14058	0.00558806	0.39454773	7.01436	25.35350
PLEKHG1	ENSG000001	3.35173	0.00608843	0.42071014	0.00000	0.00000
ZG16B	ENSG000001	2.23748	0.00613416	0.42140012	0.10469	0.16357
FGL2	ENSG000001	1.93865	0.00635251	0.42943661	0.62815	1.88107

LY86	ENSG000001	1.57261	0.00630677	0.42943661	1.25630	1.30857
C1QA	ENSG000001	3.12957	0.00676127	0.43758812	0.10469	0.00000
BCL7A	ENSG000001	1.52727	0.00678254	0.43758812	0.94223	1.88107
FADS2	ENSG000001	1.35624	0.00660807	0.43758812	2.09384	7.27891
SIGLEC7	ENSG000001	1.25948	0.00661329	0.43758812	21.04308	29.52456
CD4	ENSG000000	1.81952	0.00699447	0.44717453	0.83754	7.52426
LDHA	ENSG000001	1.11865	0.00700195	0.44717453	107.30925	284.61345
GCAT	ENSG000001	2.10959	0.00763536	0.47335478	0.20938	0.24536
CD1D	ENSG000001	2.00980	0.00750392	0.47335478	0.73284	0.32714
FAM20C	ENSG000001	0.98722	0.00762178	0.47335478	33.18735	81.29476
LYZ	ENSG000000	1.72195	0.00849599	0.51184409	105.11072	1590.07321
LXN	ENSG000000	1.56982	0.00849784	0.51184409	1.36100	4.00749
CECR6	ENSG000001	1.14609	0.00843605	0.51184409	4.92052	13.73996
NCEH1	ENSG000001	0.86580	0.00867547	0.51592288	17.06479	32.87776
H2AFY2	ENSG000000	2.38014	0.00877476	0.51869013	0.00000	0.65428
DLL4	ENSG000001	2.37037	0.00896774	0.52382676	0.00000	0.40893
CD36	ENSG000001	1.51881	0.00898823	0.52382676	1.88446	15.37567
PROCR	ENSG000001	0.89521	0.00902652	0.52382676	14.13341	21.26422
PSD3	ENSG000001	1.28883	0.00913736	0.52593734	4.71114	3.27142
MMP9	ENSG000001	1.15941	0.00914566	0.52593734	3941.33775	2495.35663
LGALS1	ENSG000001	0.87579	0.00928052	0.5280845	112.02038	206.83547
SMTNL2	ENSG000001	3.11497	0.00953704	0.53660666	0.00000	0.16357
OTUD7B	ENSG000002	1.34009	0.00971315	0.53682952	1.25630	2.94428
ACTB	ENSG000000	1.00141	0.00966644	0.53682952	768.43890	1688.95185
CD209	ENSG000000	0.94700	0.00980846	0.53730906	12.14427	28.54313
HSPB1	ENSG000001	1.22354	0.00996265	0.54341326	4.39706	18.56530
ARHGDIB	ENSG000001	1.17305	0.01014026	0.5507376	59.46503	215.50473
FSCN1	ENSG000000	0.96051	0.01029482	0.55675237	9.84104	10.55033
SYT1	ENSG000000	3.02027	0.0103769	0.55881359	0.00000	0.00000
IGFBP7	ENSG000001	1.33779	0.01071294	0.5720622	0.94223	2.94428
C6orf223	ENSG000001	1.36043	0.01093324	0.5779775	0.94223	1.63571
CTSB	ENSG000001	0.94605	0.01096015	0.5779775	1410.93338	3474.90126
RAMP1	ENSG000001	2.71212	0.011009	0.57815473	0.31408	0.00000
FRMD4A	ENSG000001	1.73066	0.01112211	0.58169078	0.31408	2.28999
ADGRE3	ENSG000001	1.18132	0.01124621	0.5833799	33.81550	50.29807
ITIH3	ENSG000001	1.83943	0.01203823	0.61197532	0.20938	0.49071
ASGR2	ENSG000001	2.64327	0.01246568	0.62372584	0.00000	0.32714
ZCWPW2	ENSG000002	2.26690	0.01241915	0.62372584	0.00000	0.00000
PROS1	ENSG000001	1.66427	0.01311228	0.62774674	0.10469	1.47214
CLDN23	ENSG000002	1.22522	0.01313877	0.62774674	5.75806	9.81426
LMNB1	ENSG000001	1.14826	0.01279842	0.62774674	2.82668	8.75105
TPI1	ENSG000001	0.84497	0.01303232	0.62774674	137.14645	244.86571
HVCN1	ENSG000001	1.35639	0.01322709	0.62959973	2.19853	9.73247
CD300LF	ENSG000001	1.17151	0.01333462	0.62999904	6.90967	25.84421

RCAN	ENSG000001	0.83268	0.0136344	0.63940792	10.88796	20.36458
WNT5A	ENSG000001	0.94188	0.01382574	0.64599737	25.64953	56.67733
SCD5	ENSG000001	2.30274	0.01394556	0.64920927	0.00000	0.16357
CLEC4G	ENSG000001	1.96864	0.0143069	0.66359974	0.10469	0.24536
CACNA2D3	ENSG000001	2.52225	0.01458153	0.67143723	0.62815	0.08179
EMILIN1	ENSG000001	1.19232	0.0145656	0.67143723	15.70379	93.48080
DTNA	ENSG000001	1.49820	0.01465858	0.67254848	0.41877	2.12642
IL4I1	ENSG000001	0.82035	0.01499244	0.68049626	78.41427	132.65604
SLA	ENSG000001	1.61453	0.01507016	0.68158956	10.15512	42.85559
AUTS2	ENSG000001	1.96100	0.01518002	0.68231083	0.20938	0.08179
CCND3	ENSG000001	1.18190	0.01519348	0.68231083	25.12607	133.47390
SLAMF1	ENSG000001	1.17236	0.01525578	0.68269603	63.33863	48.74414
NLRC5	ENSG000001	0.84648	0.0154075	0.68706621	15.28502	30.17884
ACOT11	ENSG000001	1.53742	0.01583701	0.69326097	1.04692	1.14500
PTPRO	ENSG000001	1.82226	0.01607471	0.69724739	0.62815	4.49820
TTYH2	ENSG000001	1.32919	0.01615917	0.69780891	2.40791	4.08927
STAT4	ENSG000001	1.08457	0.01625238	0.69780891	3.14076	4.98891
TNNT1	ENSG000001	2.18702	0.01683454	0.71159226	0.00000	0.49071
LDHB	ENSG000001	1.18454	0.01745499	0.71159226	2.30322	5.39784
IDO1	ENSG000001	1.05374	0.01694049	0.71159226	49.51929	188.35195
FAM200B	ENSG000002	0.85526	0.0172589	0.71159226	10.88796	14.55781
TAX1BP3	ENSG000002	0.82901	0.01675199	0.71159226	26.06829	58.06769
CERS6	ENSG000001	0.76350	0.01779676	0.72031547	21.04308	38.52096
FCGRT	ENSG000001	0.99039	0.01799161	0.7258899	61.66356	214.11437
TRAF5	ENSG000000	1.59092	0.01820957	0.73004874	1.25630	0.57250
IVD	ENSG000001	1.17211	0.01843461	0.7367468	2.09384	3.76213
COLEC12	ENSG000001	2.35582	0.01851445	0.73761797	0.31408	0.49071
LGALS2	ENSG000001	3.27418	0.01873096	0.73883498	0.10469	0.16357
DNAJC5B	ENSG000001	1.20349	0.01867298	0.73883498	1.36100	5.31606
SPARC	ENSG000001	1.19846	0.01877754	0.73883498	3.35014	3.92570
ZC4H2	ENSG000001	1.76372	0.01917057	0.74292562	0.20938	0.40893
VSIG4	ENSG000001	1.66126	0.01899894	0.74292562	0.20938	0.65428
AIF1	ENSG000002	1.12556	0.01900045	0.74292562	9.84104	39.42060
RPGRIP1	ENSG000000	2.99181	0.01963206	0.74605297	0.00000	0.32714
BUB1	ENSG000001	2.04761	0.01937284	0.74605297	0.00000	0.24536
MT1G	ENSG000001	1.44919	0.01949291	0.74605297	4.60645	22.08208
CLU	ENSG000001	1.81307	0.0200935	0.75471126	0.00000	1.63571
LINC01420	ENSG000002	1.10343	0.01996524	0.75471126	5.54867	4.82534
JAML	ENSG000001	2.50955	0.02053628	0.7609202	0.00000	6.95177
PKIB	ENSG000001	2.63401	0.02095124	0.76734671	0.00000	0.08179
PTRF	ENSG000001	1.92579	0.02085766	0.76734671	0.10469	0.24536
MT-ND6	ENSG000001	0.84084	0.02091935	0.76734671	27.32460	31.07848
FAT2	ENSG000000	2.99969	0.02119108	0.76994993	0.00000	0.08179
CRIP1	ENSG000002	1.34436	0.02120407	0.76994993	0.94223	1.47214

GLRX	ENSG000001	1.02232	0.02109464	0.76994993	38.73602	182.46339
TBX3	ENSG000001	2.70690	0.02131041	0.77160672	0.00000	0.16357
AP2S1	ENSG000000	0.71289	0.02138486	0.77210276	30.25597	57.24983
HLA-DQA2	ENSG000002	2.04901	0.02174999	0.77835372	3.76891	0.57250
FZD3	ENSG000001	1.53488	0.02186012	0.77835372	0.20938	0.65428
AK8	ENSG000001	1.50033	0.02184895	0.77835372	0.83754	1.55392
TBC1D4	ENSG000001	1.38835	0.0219867	0.77835372	1.15161	1.96285
GUCY1B3	ENSG000000	1.81479	0.02231781	0.78788066	0.10469	0.24536
C16orf45	ENSG000001	1.89354	0.02238224	0.78796648	0.41877	0.32714
ABCG1	ENSG000001	1.14178	0.02281773	0.79887203	1.46569	3.92570
GP1BA	ENSG000001	2.02337	0.02292378	0.80037996	0.10469	0.32714
BICC1	ENSG000001	2.04728	0.02316142	0.80425813	0.31408	0.08179
FAIM	ENSG000001	1.16326	0.02314381	0.80425813	1.25630	4.08927
CYFIP2	ENSG000000	1.11346	0.02325513	0.80531171	4.71114	3.10785
PROB1	ENSG000002	1.47300	0.02354	0.80856719	0.31408	0.73607
IGFLR1	ENSG000001	0.91927	0.02348949	0.80856719	18.73986	61.74803
FBXO6	ENSG000001	0.86865	0.02378223	0.81203029	6.70028	13.24925
SLCO2B1	ENSG000001	2.25573	0.02416183	0.81805855	0.00000	7.76962
RFTN1	ENSG000001	0.83614	0.024286	0.81814808	66.58408	181.15483
C10orf10	ENSG000001	2.45471	0.02451167	0.82194939	0.00000	0.16357
SLAMF9	ENSG000001	1.86200	0.02545618	0.82955512	0.31408	0.32714
S100A9	ENSG000001	1.22198	0.02488856	0.82955512	177.03408	1361.56459
CHI3L2	ENSG000000	1.21006	0.02586814	0.82955512	1.88446	7.03355
SPATS2	ENSG000001	1.14865	0.0259134	0.82955512	1.67507	5.56141
ALDOC	ENSG000001	1.07549	0.0257545	0.82955512	5.86275	7.11534
UCP2	ENSG000001	1.01340	0.02533942	0.82955512	46.27384	169.78665
DENND3	ENSG000001	0.81870	0.02570813	0.82955512	53.70697	69.51765
PLEKHG2	ENSG000000	0.80689	0.02542946	0.82955512	54.54450	74.58835
GPI	ENSG000001	0.76580	0.02579587	0.82955512	22.71815	56.35019
PSRC1	ENSG000001	1.99632	0.02668427	0.83250993	0.00000	0.24536
PLCL1	ENSG000001	1.46557	0.02724161	0.83250993	0.41877	3.43499
SPECC1	ENSG000001	1.07287	0.02724728	0.83250993	2.51261	3.68035
DBNDD2	ENSG000002	0.86537	0.02709725	0.83250993	8.06128	17.25674
PLXNC1	ENSG000001	0.84129	0.0269111	0.83250993	57.68526	139.52602
P4HA1	ENSG000001	0.76306	0.0271877	0.83250993	49.72868	87.51046
LAP3	ENSG000000	0.68831	0.02687039	0.83250993	21.77593	27.47992
IL21R	ENSG000001	2.02014	0.02852421	0.83794522	0.00000	0.89964
NDP	ENSG000001	1.90121	0.02786855	0.83794522	0.00000	2.20821
FZD2	ENSG000001	1.77635	0.02758941	0.83794522	0.31408	1.14500
CARD9	ENSG000001	1.23639	0.02798654	0.83794522	2.09384	7.44248
ATF7IP2	ENSG000001	1.16292	0.02836448	0.83794522	1.25630	4.00749
METTL1	ENSG000000	1.12986	0.02812534	0.83794522	2.09384	4.82534
LRP5	ENSG000001	1.12867	0.02843622	0.83794522	4.18768	2.45356
ANXA6	ENSG000001	1.06919	0.02860237	0.83794522	6.07213	27.47992

MT2A	ENSG000001	0.97943	0.02852209	0.83794522	193.05195	112.53681
CPM	ENSG000001	0.79663	0.02840884	0.83794522	45.64569	46.12701
C3orf14	ENSG000001	1.22939	0.02874625	0.839853	1.57038	2.86249
DOCK1	ENSG000001	0.94715	0.02887488	0.84167633	5.12991	17.42031
VASH1	ENSG000000	1.37715	0.02904584	0.84279352	2.93137	42.93737
PLBD1	ENSG000001	1.33786	0.02904437	0.84279352	2.09384	16.35710
KCTD12	ENSG000001	0.89309	0.02913993	0.84359774	36.32811	129.13927
ZHX3	ENSG000001	1.18857	0.02946888	0.84557115	1.15161	1.47214
TRPM4	ENSG000001	1.11228	0.02938135	0.84557115	2.40791	8.26033
H1F0	ENSG000001	0.87494	0.02941129	0.84557115	82.28787	212.56045
PLEKHO1	ENSG000000	0.78469	0.02961752	0.84776828	86.37086	220.00293
FPR3	ENSG000001	1.80791	0.02980912	0.84871705	3.97829	42.61023
ID3	ENSG000001	1.75670	0.03009711	0.8519023	0.20938	4.08927
KIAA1211L	ENSG000001	1.61605	0.03056839	0.85383212	0.10469	0.24536
SAMHD1	ENSG000001	1.06994	0.0305401	0.85383212	24.70730	113.51824
SPINT2	ENSG000001	0.73814	0.03040711	0.85383212	24.81199	27.23456
VMO1	ENSG000001	1.29596	0.0308848	0.85701941	0.94223	3.59856
FAM101B	ENSG000001	0.90776	0.03099482	0.85819855	15.38972	25.84421
CIITA	ENSG000001	1.33362	0.03158398	0.86695648	3.55953	39.33881
TMEM176A	ENSG000000	1.01810	0.03153408	0.86695648	11.51611	47.51736
MRC2	ENSG000000	1.49193	0.03183242	0.86899786	1.77976	0.89964
ZNF680	ENSG000001	1.49188	0.03206861	0.86899786	0.52346	0.81785
TNFRSF4	ENSG000001	0.95182	0.03199163	0.86899786	6.17682	6.29748
ZFP36L1	ENSG000001	0.79215	0.03214768	0.86928706	74.54067	183.93553
PRR11	ENSG000000	1.68672	0.03237783	0.87180057	0.20938	1.14500
C2orf74	ENSG000002	1.19690	0.03274756	0.87923147	1.25630	2.04464
NDN	ENSG000001	2.31484	0.03310932	0.88030621	0.10469	0.00000
CENPE	ENSG000001	1.48589	0.03305497	0.88030621	0.20938	1.79928
MCM6	ENSG000000	1.07850	0.03322346	0.88056582	2.40791	4.41642
VGLL4	ENSG000001	0.99922	0.03325766	0.88056582	11.62081	16.27531
IL16	ENSG000001	0.75665	0.0337626	0.88654723	45.95977	65.10124
TPCN1	ENSG000001	0.78615	0.0338552	0.88714594	14.02872	31.16027
GSPT2	ENSG000001	1.13206	0.0339335	0.88736789	1.04692	1.63571
RGS14	ENSG000001	0.87135	0.0345401	0.89350204	5.86275	13.41282
CXCR5	ENSG000001	1.73918	0.03476198	0.89506487	1.04692	1.30857
CKB	ENSG000001	0.90785	0.03499372	0.89506487	5.23460	6.21570
NR1H3	ENSG000000	1.39820	0.03519043	0.89620143	1.57038	3.68035
SLC44A2	ENSG000001	0.96540	0.03532905	0.89620143	5.44398	17.33852
GIPC3	ENSG000001	1.88330	0.03693654	0.89737299	0.00000	0.24536
HAPLN3	ENSG000001	1.63442	0.03613056	0.89737299	0.41877	0.32714
SMYD3	ENSG000001	1.53590	0.03778742	0.89737299	0.31408	0.32714
THBS2	ENSG000001	1.51068	0.03587375	0.89737299	0.41877	2.69892
MMP2	ENSG000000	1.44224	0.03728665	0.89737299	0.62815	0.73607
STMN1	ENSG000001	1.35416	0.0365167	0.89737299	0.52346	0.98143

YPEL4	ENSG000001	1.33911	0.03698169	0.89737299	2.61730	1.96285
CAMK1	ENSG000001	1.25989	0.03655905	0.89737299	1.88446	8.26033
CATIP-AS1	ENSG000002	1.25395	0.03822447	0.89737299	1.04692	0.81785
RNASE6	ENSG000001	1.19792	0.03794011	0.89737299	2.61730	3.27142
DDX11	ENSG000000	1.14820	0.03721663	0.89737299	4.71114	4.74356
LOXL2	ENSG000001	1.13386	0.03706242	0.89737299	1.36100	2.69892
SLC16A10	ENSG000001	1.07435	0.0359224	0.89737299	27.21991	18.89244
METTL21B	ENSG000001	1.04279	0.03670344	0.89737299	2.82668	10.71390
ZNF469	ENSG000002	1.00749	0.0371747	0.89737299	3.66422	6.37927
ST6GAL1	ENSG000000	0.95466	0.03841637	0.89737299	3.14076	4.41642
VAMP8	ENSG000001	0.89987	0.03757568	0.89737299	11.51611	29.52456
KCNE3	ENSG000001	0.86212	0.03797963	0.89737299	9.73635	35.57668
ARL3	ENSG000001	0.83677	0.038623	0.89737299	6.17682	13.08568
DRAM2	ENSG000001	0.76361	0.03681027	0.89737299	18.00701	43.75523
SLC11A1	ENSG000000	0.70081	0.03678966	0.89737299	478.96566	723.80145
CREBL2	ENSG000001	0.69543	0.03624458	0.89737299	54.02104	102.88613

Gene_Symbol	TSLPR⁻ 3	TSLPR⁺ 1	TSLPR⁺ 2	TSLPR⁺ 3
CCR7	0.77102	73.19829	56.11989	99.51246
CRLF2	0.71171	23.71074	31.99017	22.78857
LAMP3	9.25226	31.18798	63.15773	79.79571
MMP12	0.11862	3.34508	2.10221	3.00038
LAD1	2.49099	8.55948	29.43095	27.57488
MMP7	0.53378	3.34508	4.47862	7.00088
SORBS3	7.29505	29.12190	24.58673	29.36082
HLA-DPA1	5.75301	12.79002	17.18329	78.00977
TNNT2	0.11862	0.49192	5.39263	7.07231
CD1C	0.77102	5.21439	3.10762	8.64394
C1QC	0.05931	1.77093	0.63980	1.35731
CD86	18.74175	41.81354	29.33955	81.22446
FCRLB	7.35436	29.31867	31.99017	19.50244
GCSAM	0.00000	0.29515	0.73120	4.07194
HLA-DMA	7.05781	17.02057	15.90368	41.93382
CD1E	0.17793	1.18062	0.82260	5.85788
NCCRP1	0.05931	3.24670	1.91941	4.28625
PALLD	1.18619	4.32893	7.86044	16.71638
MRC1	90.62467	286.89007	113.88499	506.49199
FCGR2B	92.10740	215.26594	137.74052	278.24913
FBN1	0.17793	0.29515	2.01081	4.85775
CD74	22.83410	85.98831	93.13709	308.89582
HLA-DPB1	2.01652	4.72247	6.30663	36.14738
TFRC	101.71552	259.73586	383.51640	278.74919
SLC22A23	0.53378	0.98385	5.20983	7.14375
EMP2	0.23724	3.04993	2.37641	1.71450
CXCL13	0.11862	0.09838	3.47322	8.07244
CALCRL	0.23724	0.78708	1.73661	1.85738
TSPAN15	0.00000	0.19677	1.46241	0.78581
CST7	0.05931	0.29515	1.00541	4.42913
GAS6	1.18619	3.83701	4.11302	6.42938
C1QB	0.05931	1.27900	0.36560	1.00013
CLEC4F	0.29655	0.98385	0.82260	4.28625
HLA-DMB	2.78754	10.62556	5.48403	26.07469
MGAT4A	31.31533	51.75040	73.21178	94.15465
CYP2S1	10.73499	27.94128	36.65159	34.57576
NAV2	8.65916	17.41411	28.42555	17.50219
HLA-DRA	51.12465	67.39359	87.83586	332.68451
ZNF366	0.71171	0.88546	3.65602	4.85775
CYP27B1	8.48124	13.28195	57.58230	68.93720
ROBO1	0.23724	1.96770	2.92482	0.85725
MT1E	11.56532	31.58152	28.33415	66.29402

TVP23A	0.05931	0.09838	0.82260	2.85750
FBP1	16.25076	47.02793	11.42506	118.22909
GFPT2	1.66066	3.64024	11.33366	10.28700
ENTHD1	0.41517	1.67254	1.37101	2.42888
CPED1	1.12688	8.26432	3.29042	4.07194
HLA-DRB1	40.80483	51.06171	56.11989	254.38900
ENO2	15.24250	82.64323	69.55576	44.43414
ENTPD1	0.23724	0.59031	2.10221	2.14313
MT1X	16.72523	36.00884	33.90958	96.51208
ALOX15B	1.71997	11.70779	14.16707	6.71513
RTN1	8.65916	24.20266	23.58132	54.93545
EHF	0.88964	4.52570	7.76904	7.64381
ITIH1	4.80406	11.31425	18.55430	16.28775
TCF4	4.15165	10.23202	9.87125	12.07294
PTGIR	49.34537	82.84000	115.07320	96.29777
KCNE5	0.77102	2.85316	3.29042	6.07219
MT1M	5.15991	9.14979	11.97346	40.36220
CCL22	2.84685	7.77240	3.74742	15.07332
HLA-DRB5	9.37088	11.51102	13.07027	69.00864
EBI3	4.74475	54.40679	68.64176	34.71863
FPR2	15.77628	77.62560	35.18918	52.14939
HLA-DOA	0.35586	0.29515	1.37101	4.07194
GCKR	1.60135	4.42732	12.70467	5.71500
SPN	25.02854	54.89872	21.11351	73.08058
HIST1H1C	6.70196	20.66081	20.10810	25.93182
TNFRSF6B	1.83859	15.83995	14.44128	8.28675
MT1F	15.59836	29.61382	40.94741	92.51158
MOB3B	33.15392	81.06907	52.73807	75.00939
CTSH	238.95733	1212.19909	613.93700	791.67056
VEGFA	43.65167	104.97658	109.31497	58.65020
ACE	1.06757	2.85316	3.29042	8.00100
HSD11B1	0.59309	1.47577	1.09681	7.42950
LAIR1	36.53455	78.51107	123.48204	159.44854
RYR1	1.12688	2.26285	6.03243	4.50056
PLXDC2	27.81608	46.14247	50.81866	79.22421
CORO1A	29.59536	50.86494	108.03536	99.22671
CCL24	121.16898	110.09259	138.74592	925.04440
HAS1	2.13514	5.90309	2.55921	9.42975
TSPAN33	23.54581	103.59919	108.30956	91.94008
MEP1A	0.77102	3.34508	3.74742	1.71450
ITGB2	350.22165	831.44992	683.40136	1174.00414
CD1B	0.59309	1.08223	1.00541	2.92894
PARP15	1.83859	4.82086	10.69386	2.42888
SLC1A2	1.95721	3.04993	10.69386	8.35819

ADAMTS14	58.65694	112.25705	127.59507	151.66185
FLT3	0.23724	0.49192	0.73120	1.14300
PPBP	11.03154	9.14979	34.09238	54.43539
CLIC2	6.34610	15.05287	11.97346	11.93007
PECAM1	6.58334	9.05140	26.50614	26.50332
CD207	0.11862	0.59031	0.27420	0.64294
CLEC6A	0.17793	1.08223	2.01081	5.35781
RARRES1	0.00000	0.00000	1.00541	1.00013
TIAM1	30.60362	43.97800	37.38279	56.22133
CLEC10A	0.05931	1.57416	5.57543	7.42950
A2M	3.32132	21.74304	4.11302	37.50470
TMEM173	8.06607	13.57710	27.87715	20.50257
FPR1	5.87162	82.54484	33.08697	38.36195
CYGB	0.11862	0.98385	0.63980	0.92869
ITGA4	2.55030	7.57563	6.12383	7.14375
CCR6	0.11862	0.78708	0.63980	0.57150
ADCY6	0.35586	1.37739	1.55381	1.78594
PTPRF	0.59309	1.27900	7.86044	3.71475
GSN	139.02109	159.08822	114.52480	478.84567
ZNF395	13.64115	48.01178	33.36117	19.35957
ACTG1	319.55872	462.70370	391.19404	931.68809
STEAP3	22.12238	49.09401	84.63684	70.58027
TIFAB	0.29655	1.08223	4.66142	3.71475
FAM124A	8.36262	19.67696	18.91990	16.28775
LMO2	6.99850	22.43173	15.90368	21.85988
NDRG2	1.48273	0.88546	1.64521	15.00188
TNFAIP8L2	13.10736	26.07197	35.00638	35.36157
CP	0.00000	0.68869	0.54840	0.42863
HNMT	19.80932	56.86641	103.46534	77.58114
UGCG	43.94822	76.24822	79.60982	78.36696
TREM2	0.05931	0.00000	0.54840	3.64331
INSM1	0.05931	0.29515	1.09681	0.64294
C1orf54	1.71997	1.27900	2.37641	8.64394
FABP5	4.50751	4.23055	6.76364	18.00225
TNFSF13	3.02478	31.08960	17.00049	11.50144
KCP	2.66892	9.83848	2.37641	5.07206
ALDH2	1.95721	6.69017	16.17788	20.57400
SPRED1	54.20874	59.52280	65.80834	93.72602
MROH7	0.29655	1.47577	0.54840	0.42863
PPP1R14C	0.35586	1.47577	0.45700	1.00013
RAB3D	14.29355	23.02204	42.40982	35.29013
PLEKHG1	0.17793	0.00000	0.63980	1.78594
ZG16B	0.17793	0.68869	1.00541	0.57150
FGL2	2.13514	1.08223	6.30663	10.71563

LY86	1.54204	4.62409	2.01081	5.42925
C1QA	0.05931	0.59031	0.18280	0.78581
BCL7A	1.36411	3.24670	6.21523	2.64319
FADS2	12.39565	14.16741	19.65110	20.64544
SIGLEC7	8.42193	62.57273	47.34545	28.43213
CD4	2.60961	3.73862	17.64029	16.78782
LDHA	138.07214	477.06788	382.14539	240.38724
GCAT	0.41517	0.68869	0.63980	2.57175
CD1D	0.23724	1.86931	2.28501	1.00013
FAM20C	63.46099	107.33781	75.86240	158.66272
LYZ	515.81332	1178.05956	2289.12493	3523.22687
LXN	1.18619	3.24670	6.76364	9.28688
CECR6	6.16817	19.38181	15.53808	18.14513
NCEH1	35.22975	39.05876	56.02849	58.07870
H2AFY2	0.29655	0.29515	1.82801	3.00038
DLL4	0.05931	0.39354	0.73120	1.35731
CD36	6.16817	10.23202	23.30712	31.78969
PROCR	16.07283	31.67990	25.40933	37.07607
PSD3	8.06607	18.10280	11.15086	9.21544
MMP9	3682.22032	9469.33995	3620.92128	9371.88778
LGALS1	133.80187	262.49064	250.52871	301.10913
SMTNL2	0.00000	0.09838	1.00541	0.50006
OTUD7B	4.27027	4.91924	6.85504	9.57263
ACTB	1142.83166	1631.02317	2022.32694	3454.93261
CD209	18.38590	38.46846	27.87715	44.00551
HSPB1	13.40391	24.89135	17.09189	39.57638
ARHGDIIB	166.89648	223.43187	215.33952	527.70893
FSCN1	9.72673	16.92219	17.00049	24.64594
SYT1	0.11862	0.68869	0.00000	0.64294
IGFBP7	2.60961	3.73862	6.30663	6.28650
C6orf223	1.77928	2.36124	4.20442	4.71488
CTSB	2730.54267	4791.53639	4164.66271	5224.72564
RAMP1	0.41517	0.88546	0.18280	4.00050
FRMD4A	2.55030	1.86931	6.48943	8.78681
ADGRE3	18.62313	111.96190	81.25502	32.93270
ITIH3	0.77102	0.49192	2.01081	3.00038
ASGR2	0.00000	1.08223	0.63980	0.35719
ZCWPW2	0.35586	0.29515	0.73120	1.07156
PROS1	0.88964	1.47577	3.29042	3.07181
CLDN23	12.81082	16.23349	10.05405	39.07632
LMNB1	5.27853	8.46109	13.43587	14.85900
TPII	182.13898	361.07221	283.06728	342.32858
HVCN1	6.82057	8.75625	10.60246	27.57488
CD300LF	15.89490	16.52865	33.08697	58.29301

RCAN	19.57208	27.15420	30.61916	31.14676
WNT5A	40.27104	99.07349	85.00244	42.07670
SCD5	0.17793	0.19677	0.63980	1.07156
CLEC4G	0.17793	0.49192	0.73120	0.92869
CACNA2D3	0.11862	3.14831	0.54840	0.85725
EMILIN1	87.54058	98.18803	141.94494	193.38136
DTNA	3.02478	3.83701	3.83882	7.85813
IL4I1	84.27857	184.37311	144.77835	180.66548
SLA	7.05781	11.11748	87.83586	85.08208
AUTS2	0.23724	0.49192	0.73120	0.92869
CCND3	55.75078	80.18361	186.18277	208.24036
SLAMF1	20.75827	141.37895	111.14298	47.64882
NLRC5	18.56382	32.56537	50.63586	30.50382
ACOT11	2.96547	5.11601	1.91941	7.78669
PTPRO	3.49925	1.37739	11.05946	18.00225
TTYH2	1.24550	4.82086	8.86585	5.71500
STAT4	6.99850	12.49487	9.04865	9.78694
TNNT1	0.47447	0.49192	0.63980	3.42900
LDHB	2.60961	5.80470	7.22064	10.07269
IDO1	149.28161	134.29525	319.71887	335.18483
FAM200B	10.37913	19.18504	22.21032	23.07432
TAX1BP3	40.09311	52.53748	60.87272	103.79871
CERS6	35.76353	46.43762	46.70564	65.79395
FCGRT	80.95725	181.02803	216.61913	290.67925
TRAF5	1.54204	1.27900	2.92482	6.28650
IVD	3.73649	5.31278	5.48403	10.64419
COLEC12	0.77102	0.19677	0.82260	7.35806
LGALS2	3.02478	1.47577	0.09140	30.64669
DNAJC5B	4.27027	5.80470	10.23685	8.78681
SPARC	1.71997	5.11601	8.04324	7.57238
ZC4H2	0.23724	0.59031	1.37101	1.00013
VSIG4	0.59309	0.78708	1.18821	2.71463
AIF1	16.42869	19.38181	54.93169	67.22270
RPGRIP1	0.00000	0.00000	2.01081	0.78581
BUB1	0.11862	0.59031	0.54840	0.50006
MT1G	38.37314	26.36713	29.88796	116.94321
CLU	0.71171	1.96770	1.64521	4.42913
LINC01420	8.54054	10.52717	8.68305	21.50269
JAML	1.95721	1.08223	11.24226	37.07607
PKIB	0.77102	0.49192	0.27420	4.92919
PTRF	0.29655	1.18062	0.45700	0.92869
MT-ND6	31.37464	41.22323	87.01325	34.00426
FAT2	0.05931	0.68869	0.73120	0.00000
CRIP1	1.60135	1.57416	3.38182	5.35781

GLRX	93.53083	135.47587	226.85598	258.10375
TBX3	0.94895	0.29515	0.45700	6.92944
AP2S1	39.26278	56.37449	69.00736	79.58139
HLA-DQA2	0.94895	12.88841	0.91400	8.35819
FZD3	0.41517	1.08223	1.46241	1.21444
AK8	5.04129	5.80470	3.56462	11.35857
TBC1D4	2.01652	1.57416	4.38722	7.64381
GUCY1B3	0.29655	0.59031	0.82260	1.00013
C16orf45	0.17793	0.29515	1.27961	1.85738
ABCG1	2.31306	4.62409	5.30123	6.78656
GP1BA	0.29655	1.96770	0.45700	0.57150
BICC1	0.17793	0.78708	1.27961	0.35719
FAIM	4.80406	5.80470	9.14005	7.50094
CYFIP2	2.60961	6.78855	7.67764	8.35819
PROB1	0.53378	1.08223	1.64521	1.71450
IGFLR1	42.93996	45.65055	65.07714	117.87190
FBXO6	9.31157	18.20119	16.63489	17.35932
SLCO2B1	2.60961	2.06608	12.24766	33.86138
RFTN1	93.17497	176.89587	238.73804	177.45079
C10orf10	0.05931	0.00000	0.82260	0.57150
SLAMF9	2.01652	0.78708	2.28501	6.92944
S100A9	515.75401	824.56298	1736.51765	2072.54523
CHI3L2	3.49925	4.42732	10.78526	13.21594
SPATS2	2.90616	4.62409	8.86585	8.71538
ALDOC	3.49925	15.54480	9.04865	9.35831
UCP2	78.88142	91.69463	221.64616	273.60569
DENND3	46.32059	138.62418	87.47026	64.65095
PLEKHG2	34.99251	100.45088	118.54642	66.15114
GPI	49.70123	81.26584	59.77591	69.29439
PSRC1	0.11862	0.29515	0.63980	0.64294
PLCL1	1.71997	1.96770	6.85504	6.42938
SPECC1	3.79580	4.32893	6.58083	10.14413
DBNDD2	11.56532	14.16741	24.67813	27.86063
PLXNC1	52.25153	140.49349	155.83781	139.66034
P4HA1	53.20048	132.62271	100.44912	80.15289
LAP3	29.71398	39.35392	37.93120	48.72039
IL21R	0.17793	0.29515	1.82801	2.28600
NDP	2.84685	1.27900	8.50024	9.07256
FZD2	0.11862	0.78708	3.10762	1.50019
CARD9	4.80406	4.42732	9.68845	19.35957
ATF7IP2	1.95721	5.80470	5.39263	4.50056
METTL1	4.74475	4.42732	7.86044	13.14450
LRP5	2.78754	8.46109	7.03784	5.14350
ANXA6	12.03980	14.26580	37.29139	42.50532

MT2A	126.38820	273.80489	139.93413	453.62823
CPM	34.99251	101.33634	50.08746	64.36520
C3orf14	1.66066	6.98532	3.65602	3.14325
DOCK1	12.39565	14.36418	29.52235	22.35994
VASH1	9.43018	26.76066	58.49630	52.36370
PLBD1	15.00526	12.59325	17.91449	51.64932
KCTD12	76.09388	92.67848	145.69236	199.95361
ZHX3	1.06757	3.34508	2.74201	2.21456
TRPM4	4.56682	8.16594	17.09189	7.14375
H1F0	143.05413	148.95458	245.68448	398.69278
PLEKHO1	148.45128	200.01629	249.52330	316.96826
FPR3	110.84915	58.34218	70.92677	406.69378
ID3	0.65240	1.86931	7.40344	7.07231
KIAA1211L	0.41517	0.88546	0.91400	0.71438
SAMHD1	101.12242	75.06760	155.38081	261.17556
SPINT2	15.71697	34.82822	38.02260	40.50507
VMO1	1.18619	2.85316	6.76364	4.28625
FAM101B	11.15016	42.69900	33.17837	19.57388
CIITA	16.48800	15.83995	55.48009	74.43789
TMEM176A	42.22825	31.77829	57.49090	111.65684
MRC2	2.72823	7.47724	1.37101	6.07219
ZNF680	0.29655	1.57416	1.27961	1.64306
TNFRSF4	5.57508	15.24964	9.32285	9.71550
ZFP36L1	144.35893	265.93411	181.70415	220.74193
PRR11	0.29655	0.49192	3.01622	1.85738
C2orf74	3.38063	2.75477	4.66142	8.00100
NDN	0.17793	0.68869	0.00000	0.85725
CENPE	0.65240	1.18062	3.74742	2.50031
MCM6	6.28679	6.69017	6.48943	14.21607
VGLL4	6.28679	29.12190	25.77493	12.14438
IL16	40.62690	114.12636	76.50220	58.50733
TPCN1	13.81908	27.05582	39.85061	33.43276
GSPT2	2.13514	4.03378	2.46781	3.92906
RGS14	7.82883	11.60941	16.63489	20.71688
CXCR5	2.13514	9.93686	0.45700	3.71475
CKB	10.31983	8.55948	14.98968	17.50219
NR1H3	4.92268	2.26285	6.03243	18.64519
SLC44A2	7.23574	15.83995	27.42014	14.07319
GIPC3	0.35586	0.19677	0.63980	1.57163
HAPLN3	0.23724	1.47577	0.73120	0.78581
SMYD3	0.29655	0.68869	1.37101	0.71438
THBS2	1.00826	1.67254	7.86044	2.21456
MMP2	2.01652	2.45962	1.18821	5.57213
STMN1	0.65240	1.77093	1.09681	2.57175

YPEL4	5.39715	5.80470	3.01622	16.50207
CAMK1	13.52253	11.51102	9.59705	34.00426
CATIP-AS1	1.00826	1.37739	2.10221	3.42900
RNASE6	8.77778	9.05140	5.11843	19.00238
DDX11	2.55030	13.28195	8.04324	4.71488
LOXL2	1.42342	2.45962	3.93022	5.57213
SLC16A10	5.75301	46.92955	38.47960	25.43176
METTL21B	6.52403	7.28047	13.89287	19.50244
ZNF469	3.14339	9.24817	10.69386	6.14363
ST6GAL1	5.27853	8.36271	6.21523	9.92981
VAMP8	17.31833	15.54480	38.84520	54.14964
KCNE3	29.41743	30.20413	38.38820	63.65083
ARL3	8.95571	11.21587	17.36609	21.35982
DRAM2	36.17870	31.38475	61.42112	71.86614
SLC11A1	682.11671	871.68930	946.81754	1209.50859
CREBL2	53.73426	89.62855	134.45010	113.94284

Supplementary Tables I and II. List of the top 500 genes that are differentially expressed in TSLPR+ and TSLPR- mono. Individual gene information are shown for each pair of TSLPR+ and TSLPR- mono. Table I, upregulated gene transcripts in TSLPR- vs TSLPR+ mono. Table II, upregulated gene transcripts in TSLPR+ vs TSLPR- mono.

6. References

1. Ziegler, S. F. 2012. Thymic stromal lymphopoietin and allergic disease. *J Allergy Clin Immunol* 130: 845-852.
2. Romeo, M. J., R. Agrawal, A. Pomes, and J. A. Woodfolk. 2014. A molecular perspective on TH2-promoting cytokine receptors in patients with allergic disease. *J Allergy Clin Immunol* 133: 952-960.
3. Arima, K., N. Watanabe, S. Hanabuchi, M. Chang, S. C. Sun, and Y. J. Liu. 2010. Distinct signal codes generate dendritic cell functional plasticity. *Sci Signal* 3: ra4.
4. Bell, B. D., M. Kitajima, R. P. Larson, T. A. Stoklasek, K. Dang, K. Sakamoto, K. U. Wagner, D. H. Kaplan, B. Reizis, L. Hennighausen, and S. F. Ziegler. 2013. The transcription factor STAT5 is critical in dendritic cells for the development of TH2 but not TH1 responses. *Nat Immunol* 14: 364-371.
5. Lo Kuan, E., and S. F. Ziegler. 2014. Thymic stromal lymphopoietin and cancer. *J Immunol* 193: 4283-4288.
6. Volpe, E., L. Pattarini, C. Martinez-Cingolani, S. Meller, M. H. Donnadieu, S. I. Bogiatzi, M. I. Fernandez, M. Touzot, J. C. Bichet, F. Reyal, M. P. Paronetto, A. Chiricozzi, S. Chimenti, F. Nasorri, A. Cavani, A. Kislat, B. Homey, and V. Soumelis. 2014. Thymic stromal lymphopoietin links keratinocytes and dendritic cell-derived IL-23 in patients with psoriasis. *J Allergy Clin Immunol* 134: 373-381.
7. Watanabe, N., S. Hanabuchi, M. A. Marloie-Provost, S. Antonenko, Y. J. Liu, and V. Soumelis. 2005. Human TSLP promotes CD40 ligand-induced IL-12 production by myeloid dendritic cells but maintains their Th2 priming potential. *Blood* 105: 4749-4751.
8. Hillen, M. R., T. R. Radstake, C. E. Hack, and J. A. van Roon. 2015. Thymic stromal lymphopoietin as a novel mediator amplifying immunopathology in rheumatic disease. *Rheumatology (Oxford)* 54: 1771-1779.
9. Piliponsky, A. M., A. Lahiri, P. Truong, M. Clauson, N. J. Shubin, H. Han, and S. F. Ziegler. 2016. Thymic Stromal Lymphopoietin Improves Survival and Reduces Inflammation in Sepsis. *Am J Respir Cell Mol Biol*.
10. Reche, P. A., V. Soumelis, D. M. Gorman, T. Clifford, M. Liu, M. Travis, S. M. Zurawski, J. Johnston, Y. J. Liu, H. Spits, R. de Waal Malefyt, R. A. Kastelein, and J. F. Bazan. 2001. Human thymic stromal lymphopoietin preferentially stimulates myeloid cells. *J Immunol* 167: 336-343.

11. Gordon, S., and F. O. Martinez. 2010. Alternative activation of macrophages: mechanism and functions. *Immunity* 32: 593-604.
12. Sica, A., and A. Mantovani. 2012. Macrophage plasticity and polarization: in vivo veritas. *J Clin Invest* 122: 787-795.
13. Han, H., M. B. Headley, W. Xu, M. R. Comeau, B. Zhou, and S. F. Ziegler. 2013. Thymic stromal lymphopoietin amplifies the differentiation of alternatively activated macrophages. *J Immunol* 190: 904-912.
14. Borriello, F., M. Longo, R. Spinelli, A. Pecoraro, F. Granata, R. I. Staiano, S. Loffredo, G. Spadaro, F. Beguinot, J. Schroeder, and G. Marone. 2015. IL-3 synergises with basophil-derived IL-4 and IL-13 to promote the alternative activation of human monocytes. *Eur J Immunol* 45: 2042-2051.
15. Janeway, C. A., P. Travers, M. Walport, and M. Shlomchik. 2001. The Immune System in Health and Disease. *Immunobiology*. 5th edition
16. Glass, C. K., and G. Natoli. 2016. Molecular control of activation and priming in macrophages. *Nat Immunol* 17: 26–33.
17. Netea, M. G., L. A. Joosten, E. Latz, K. H. Mills, G. Natoli, H. G. Stunnenberg, L. A. O'Neill, and R. J. Xavier. 2016. Trained immunity: a program of innate immune memory in health and disease. *Science*. 352: 5.
18. Borriello, F., R. Iannone, S. Di Somma, S. Loffredo, E. Scamardella, M. R. Galdiero, G. Varricchi, F. Granata, G. Portella, and G. Marone. 2017. GM-CSF and IL-3 Modulate Human Monocyte TNF- α Production and Renewal in In Vitro Models of Trained Immunity. *Front. Immunol.* 7:680.
19. Mogensen, T. H. 2009. Pathogen Recognition and Inflammatory Signaling in Innate Immune Defenses. *Clin Microbiol Rev.* 22: 240–273.
20. Chow, J.C., D. W. Young, D. T. Golenbock, W. J. Christ, and F. Gusovsky. 1999. Toll-like Receptor-4 Mediates Lipopolysaccharide-induced Signal Transduction. *The Journal Of Biological Chemistry*. 274: 10689–10692.
21. Dranoff, G. 2004. Cytokines in cancer pathogenesis and cancer therapy. *Nature Reviews Cancer*. 4: 11-22.
22. Geissmann, F., M. G. Manz, S. Jung, M. H. Sieweke, M. Merad, and K. Ley. 2010. Development of monocytes, macrophages, and dendritic cells. *Science*. 327: 656-61.
23. Ingersoll, M. A., R. Spanbroek, C. Lottaz, E. L. Gautier, M. Frankenberger, R. Hoffmann, R. Lang, M. Haniffa, M. Collin, F. Tacke, A. J. Habenicht, L. Ziegler-

- Heitbrock, and G. J. Randolph. 2010. Comparison of gene expression profiles between human and mouse monocyte subsets. *Blood*. 115: 10–19
24. Randolph, G. J., S. Beaulieu, S. Lebecque, R. M. Steinman, and W. A. Muller. 1998. Differentiation of monocytes into dendritic cells in a model of transendothelial trafficking. *Science*. 282: 480–483
25. Jakubzick, C. V., G. J. Randolph, and P. M. Henson. 2017. Monocyte differentiation and antigen-presenting functions. *Nat Rev Immunol*. 17: 349–362
26. Haniffa, M., A. Shin, V. Bigley, N. McGovern, P. Teo, P. See, P. S. Wasan, X. N. Wang, F. Malinarich, B. Malleret, A. Larbi, P. Tan, H. Zhao, M. Poidinger, S. Pagan, S. Cookson, R. Dickinson, I. Dimmick, R. F. Jarrett, L. Renia, J. Tam, C. Song, J. Connolly, J. K. Chan, A. Gehring, A. Bertoletti, M. Collin, and F. Ginhoux. 2012. Human tissues contain CD141hi cross-presenting dendritic cells with functional homology to mouse CD103+ nonlymphoid dendritic cells. *Immunity*. 37: 60–73.
27. Watchmaker, P. B., K. Lahl, M. Lee, D. Baumjohann, J. Morton, S. J. Kim, R. Zeng, A. Dent, K. M. Ansel, B. Diamond, H. Hadeiba, and E. C. Butcher. 2014. Comparative transcriptional and functional profiling defines conserved programs of intestinal DC differentiation in humans and mice. *Nature Immunol*. 15: 98–108.
28. Kim, K. W., A. Vallon-Eberhard, E. Zigmond, J. Farache, E. Shezen, G. Shakhar, A. Ludwig, S. A. Lira, and S. Jung. 2011. In vivo structure/function and expression analysis of the CX3C chemokine fractalkine. *Blood*. 118:156–167.
29. Rescigno, M., M. Urbano, B. Valzasina, M. Francolini, G. Rotta, R. Bonasio, F. Granucci, J. P. Kraehenbuhl, and P. Ricciardi-Castagnoli. 2001. Dendritic cells express tight junction proteins and penetrate gut epithelial monolayers to sample bacteria. *Nature Immunol*. 2: 361–367.
30. Guilliams, M., F. Ginhoux, C. Jakubzick, S. H. Naik, N. Onai, B. U. Schraml, E. Segura, R. Tussiwand, and S. Yona. 2014. Dendritic cells, monocytes and macrophages:a unified nomenclature based on ontogeny. *Nat Rev Immunol*. 14: 571–578.
31. Cianferoni, A., and J. Spergel. 2014. The importance of TSLP in allergic disease and its role as a potential therapeutic target. *Expert Rev Clin Immunol*. 10: 1463–1474.
32. Shochat, C., N. Tal, O. R. Bandapalli, C. Palmi, I. Ganmore, G. te Kronnie, G. Cario, G. Cazzaniga, A. E. Kulozik, M. Stanulla, M. Schrappe, A. Biondi, G. Basso, D. Bercovich, M. U. Muckenthaler, and S. Izraeli. 2011. Gain-of-function mutations in

- interleukin-7 receptor-alpha (IL7R) in childhood acute lymphoblastic leukemias. *J Exp Med.* 208: 901–908.
33. Ziegler, S. F., F. Roan, B. D. Bell, T. A. Stoklasek, M. Kitajima, and H. Han. 2013. The biology of thymic stromal lymphopoitin (TSLP). *Adv Pharmacol.* 66: 129–155
 34. NCT02340234. 2015. A study of lebrikizumab in patients with persistent moderate to severe atopic dermatitis. <https://clinicaltrials.gov/ct2/show/NCT02340234>. Accessed 4 Jan 2017
 35. Gauvreau, G. M., P. M. O'Byrne, L. P. Boulet, Y. Wang, D. Cockcroft, J. Bigler, J. M. FitzGerald, M. Boedigheimer, B. E. Davis, C. Dias, K. S. Gorski, L. Smith, E. Bautista, M. R. Comeau, R. Leigh, and J. R. Parnes. 2014. Effects of an anti-TSLP antibody on allergen-induced asthmatic responses. *N Engl J Med.* 370: 2102–2110.
 36. Canonica, G. W., G. Senna, P. D. Mitchell, P. M. O'Byrne, G. Passalacqua, and G. Varricchi. 2016. Therapeutic interventions in severe asthma. *World Allergy Organization Journal.* 9: 40-52
 37. Bolger, A. M., M. Lohse, and B. Usadel. 2014. Trimmomatic: a flexible trimmer for Illumina sequence data. *Bioinformatics* 30: 2114-2120.
 38. Dobin, A., C. A. Davis, F. Schlesinger, J. Drenkow, C. Zaleski, S. Jha, P. Batut, M. Chaisson, and T. R. Gingeras. 2013. STAR: ultrafast universal RNA-seq aligner. *Bioinformatics* 29: 15-21.
 39. Li, H., B. Handsaker, A. Wysoker, T. Fennell, J. Ruan, N. Homer, G. Marth, G. Abecasis, R. Durbin, and S. Genome Project Data Processing. 2009. The Sequence Alignment/Map format and SAMtools. *Bioinformatics* 25: 2078-2079.
 40. Delhomme, N., I. Padoleau, E. E. Furlong, and L. M. Steinmetz. 2012. easyRNASeq: a bioconductor package for processing RNA-Seq data. *Bioinformatics* 28: 2532-2533.
 41. Liao, Y., G. K. Smyth, and W. Shi. 2014. featureCounts: an efficient general purpose program for assigning sequence reads to genomic features. *Bioinformatics* 30: 923-930.
 42. Robinson, M. D., D. J. McCarthy, and G. K. Smyth. 2010. edgeR: a Bioconductor package for differential expression analysis of digital gene expression data. *Bioinformatics* 26: 139-140.
 43. Huang da, W., B. T. Sherman, and R. A. Lempicki. 2009. Systematic and integrative analysis of large gene lists using DAVID bioinformatics resources. *Nat Protoc* 4: 44-57.

44. Chu, V. T., R. Gottardo, A. E. Raftery, R. E. Bumgarner, and K. Y. Yeung. 2008. MeV+R: using MeV as a graphical user interface for Bioconductor applications in microarray analysis. *Genome Biol* 9: R118.
45. Wong, K. L., W. H. Yeap, J. J. Tai, S. M. Ong, T. M. Dang, and S. C. Wong. 2012. The three human monocyte subsets: implications for health and disease. *Immunol Res* 53: 41-57.
46. Hofer, T. P., A. M. Zawada, M. Frankenberger, K. Skokann, A. A. Satzl, W. Gesierich, M. Schuberth, J. Levin, A. Danek, B. Rotter, G. H. Heine, and L. Ziegler-Heitbrock. 2015. slan-defined subsets of CD16-positive monocytes: impact of granulomatous inflammation and M-CSF receptor mutation. *Blood* 126: 2601-2610.
47. Miazgowicz, M. M., M. S. Elliott, J. S. Debley, and S. F. Ziegler. 2013. Respiratory syncytial virus induces functional thymic stromal lymphopoietin receptor in airway epithelial cells. *J Inflamm Res* 6: 53-61.
48. Lee, H. C., and S. F. Ziegler. 2007. Inducible expression of the proallergic cytokine thymic stromal lymphopoietin in airway epithelial cells is controlled by NFkappaB. *Proc Natl Acad Sci U S A* 104: 914-919.
49. Lee, H. C., M. B. Headley, Y. M. Loo, A. Berlin, M. Gale, Jr., J. S. Debley, N. W. Lukacs, and S. F. Ziegler. 2012. Thymic stromal lymphopoietin is induced by respiratory syncytial virus-infected airway epithelial cells and promotes a type 2 response to infection. *J Allergy Clin Immunol* 130: 1187-1196 e1185.
50. Hui, C. C., S. Rusta-Sallehy, I. Asher, D. Heroux, and J. A. Denburg. 2014. The effects of thymic stromal lymphopoietin and IL-3 on human eosinophil-basophil lineage commitment: Relevance to atopic sensitization. *Immun Inflamm Dis* 2: 44-55.
51. Morris, M. C., E. A. Gilliam, and L. Li. 2014. Innate immune programing by endotoxin and its pathological consequences. *Front Immunol* 5: 680.
52. Pello, O. M., M. De Pizzol, M. Mirolo, L. Soucek, L. Zammataro, A. Amabile, A. Doni, M. Nebuloni, L. B. Swigart, G. I. Evan, A. Mantovani, and M. Locati. 2012. Role of c-MYC in alternative activation of human macrophages and tumor-associated macrophage biology. *Blood* 119: 411-421.
53. Odegaard, J. I., R. R. Ricardo-Gonzalez, M. H. Goforth, C. R. Morel, V. Subramanian, L. Mukundan, A. Red Eagle, D. Vats, F. Brombacher, A. W. Ferrante, and A. Chawla. 2007. Macrophage-specific PPARgamma controls alternative activation and improves insulin resistance. *Nature* 447: 1116-1120.

54. Bouhlel, M. A., B. Derudas, E. Rigamonti, R. Dievart, J. Brozek, S. Haulon, C. Zawadzki, B. Jude, G. Torpier, N. Marx, B. Staels, and G. Chinetti-Gbaguidi. 2007. PPARgamma activation primes human monocytes into alternative M2 macrophages with anti-inflammatory properties. *Cell Metab* 6: 137-143.
55. Liao, X., N. Sharma, F. Kapadia, G. Zhou, Y. Lu, H. Hong, K. Paruchuri, G. H. Mahabeleshwar, E. Dalmas, N. Venteclef, C. A. Flask, J. Kim, B. W. Doreian, K. Q. Lu, K. H. Kaestner, A. Hamik, K. Clement, and M. K. Jain. 2011. Kruppel-like factor 4 regulates macrophage polarization. *J Clin Invest* 121: 2736-2749.
56. Dzionaek, A., A. Fuchs, P. Schmidt, S. Cremer, M. Zysk, S. Miltenyi, D. W. Buck, and J. Schmitz. 2000. BDCA-2, BDCA-3, and BDCA-4: three markers for distinct subsets of dendritic cells in human peripheral blood. *J Immunol* 165: 6037-6046.
57. MacDonald, K. P., D. J. Munster, G. J. Clark, A. Dzionaek, J. Schmitz, and D. N. Hart. 2002. Characterization of human blood dendritic cell subsets. *Blood* 100: 4512-4520.
58. Guilliams, M., F. Ginhoux, C. Jakubzick, S. H. Naik, N. Onai, B. U. Schraml, E. Segura, R. Tussiwand, and S. Yona. 2014. Dendritic cells, monocytes and macrophages: a unified nomenclature based on ontogeny. *Nat Rev Immunol* 14: 571-578.
59. van der Meer, J. H., T. van der Poll, and C. van 't Veer. 2014. TAM receptors, Gas6, and protein S: roles in inflammation and hemostasis. *Blood* 123: 2460-2469.
60. Serhan, C. N. 2005. Lipoxins and aspirin-triggered 15-epi-lipoxins are the first lipid mediators of endogenous anti-inflammation and resolution. *Prostaglandins Leukot Essent Fatty Acids* 73: 141-162.
61. Guilliams, M., P. Bruhns, Y. Saeys, H. Hammad, and B. N. Lambrecht. 2014. The function of Fcgamma receptors in dendritic cells and macrophages. *Nat Rev Immunol* 14: 94-108.
62. Meynard, L. 2008. The inhibitory collagen receptor LAIR-1 (CD305). *J Leukoc Biol* 83: 799-803.
63. Shalova, I. N., J. Y. Lim, M. Chittezhath, A. S. Zinkernagel, F. Beasley, E. Hernandez-Jimenez, V. Toledano, C. Cubillos-Zapata, A. Rapisarda, J. Chen, K. Duan, H. Yang, M. Poidinger, G. Melillo, V. Nizet, F. Arnalich, E. Lopez-Collazo, and S. K. Biswas. 2015. Human monocytes undergo functional re-programming during sepsis mediated by hypoxia-inducible factor-1alpha. *Immunity* 42: 484-498.

64. Tay, S., J. J. Hughey, T. K. Lee, T. Lipniacki, S. R. Quake, and M. W. Covert. 2010. Single-cell NF-kappaB dynamics reveal digital activation and analogue information processing. *Nature* 466: 267-271.
65. Shalek, A. K., R. Satija, X. Adiconis, R. S. Gertner, J. T. Gaublomme, R. Raychowdhury, S. Schwartz, N. Yosef, C. Malboeuf, D. Lu, J. J. Trombetta, D. Gennert, A. Gnirke, A. Goren, N. Hacohen, J. Z. Levin, H. Park, and A. Regev. 2013. Single-cell transcriptomics reveals bimodality in expression and splicing in immune cells. *Nature* 498: 236-240.
66. Helft, J., J. Bottcher, P. Chakravarty, S. Zelenay, J. Huotari, B. U. Schraml, D. Goubau, and C. Reis e Sousa. 2015. GM-CSF Mouse Bone Marrow Cultures Comprise a Heterogeneous Population of CD11c(+)MHCII(+) Macrophages and Dendritic Cells. *Immunity* 42: 1197-1211.
67. Netea, M. G., L. A. Joosten, E. Latz, K. H. Mills, G. Natoli, H. G. Stunnenberg, L. A. O'Neill, and R. J. Xavier. 2016. Trained immunity: A program of innate immune memory in health and disease. *Science* 352: aaf1098.
68. Glass, C. K., and G. Natoli. 2016. Molecular control of activation and priming in macrophages. *Nat Immunol* 17: 26-33.
69. Segura, E., and S. Amigorena. 2013. Inflammatory dendritic cells in mice and humans. *Trends Immunol* 34: 440-445.
70. Segura, E., M. Touzot, A. Bohineust, A. Cappuccio, G. Chiocchia, A. Hosmalin, M. Dalod, V. Soumelis, and S. Amigorena. 2013. Human inflammatory dendritic cells induce Th17 cell differentiation. *Immunity* 38: 336-348.
71. Schroder, M., G. R. Melum, O. J. Landsverk, A. Bujko, S. Yaquib, E. Gran, H. Aamodt, E. S. Baekkevold, F. L. Jahnsen, and L. Richter. 2016. CD1c-Expression by Monocytes - Implications for the Use of Commercial CD1c+ Dendritic Cell Isolation Kits. *PLoS One* 11: e0157387.
72. Bakdash, G., S. I. Buschow, M. Gorris, A. Halilovic, S. V. Hato, A. E. Skold, G. Schreibelt, S. P. Sittig, R. Torensma, T. Duiveman-de Boer, C. Schroder, E. L. Smits, C. G. Figdor, and I. J. de Vries. 2016. Expansion of a BDCA1⁺CD14⁺ myeloid cell population in melanoma patients may attenuate the efficacy of dendritic cell vaccines. *Cancer Res.*
73. Loges, S., T. Schmidt, M. Tjwa, K. van Geyte, D. Lievens, E. Lutgens, D. Vanhoutte, D. Borgel, S. Plaisance, M. Hoylaerts, A. Luttun, M. Dewerchin, B. Jonckx, and P.

- Carmeliet. 2010. Malignant cells fuel tumor growth by educating infiltrating leukocytes to produce the mitogen Gas6. *Blood* 115: 2264-2273.
74. Olde Nordkamp, M. J., M. van Eijk, R. T. Urbanus, L. Bont, H. P. Haagsman, and L. Meyارد. 2014. Leukocyte-associated Ig-like receptor-1 is a novel inhibitory receptor for surfactant protein D. *J Leukoc Biol* 96: 105-111.
75. Son, M., and B. Diamond. 2014. C1q-mediated repression of human monocytes is regulated by leukocyte-associated Ig-like receptor 1 (LAIR-1). *Mol Med* 20: 559-568.
76. Son, M., F. Santiago-Schwarz, Y. Al-Abed, and B. Diamond. 2012. C1q limits dendritic cell differentiation and activation by engaging LAIR-1. *Proc Natl Acad Sci U S A* 109: 3160-3167.
77. Ziegler-Heitbrock, L., P. Ancuta, S. Crowe, M. Dalod, V. Grau, D. N. Hart, P. J. Leenen, Y. J. Liu, G. MacPherson, G. J. Randolph, J. Scherberich, J. Schmitz, K. Shortman, S. Sozzani, H. Strobl, M. Zembala, J. M. Austyn, M. B. Lutz. 2010. Nomenclature of monocytes and dendritic cells in blood. *Blood*. 116: 74-80.
78. Ziegler, S. F. 2012. Thymic stromal lymphopoietin and allergic disease. *J Allergy Clin Immunol*. 130: 845-852.